Received: 29 November 2023 | Revised: 30 April 2024 | Accepted: 13 May 2024

DOI: 10.1002/eqe.4153

RESEARCH ARTICLE

WILEY

# Probabilistic generation of hazard-consistent suites of fully non-stationary seismic records

**Hera Yanni**[1] | **Michalis Fragiadakis**[1] | **Ioannis P. Mitseas**[1,2]

[1]School of Civil Engineering, National Technical University of Athens, Athens, Greece

[2]School of Civil Engineering, University of Leeds, Leeds, UK

**Correspondence**
Michalis Fragiadakis, School of Civil Engineering, National Technical University of Athens, Iroon Politechniou 9, Athens 15772, Greece.
Email: mfrag@mail.ntua.gr

**Funding information**
Hellenic Foundation for Research and Innovation (H.F.R.I), Grant/Award Number: (ProjectNumber1261)

**Abstract**

A novel, practical, and computationally efficient probabilistic methodology for the stochastic generation of suites of fully non-stationary artificial accelerograms is presented. The proposed methodology ensures that the produced ground motion suites match a given target spectral mean and target variability for the whole period range of interest. This is achieved by first producing an ensemble of random target spectra with the given mean and variability and then using them to generate artificial, target spectrum-compatible, acceleration time-histories with spectral representation techniques. Spectral correlation can also be assumed for the generated ground motion spectra. Based on the same backbone, two different formulations are proposed for generating spectrum-compatible acceleration time-histories of the non-stationary kind. The distinction between these two variants lies in the techniques employed for modeling the temporal and spectral modulation, focusing on the site-compatibility of the produced records. The first approach uses past-recorded seismic accelerograms as seed records, and the second proposes and uses a new, probabilistic time-frequency modulating function. The outcome of the proposed methodology is suites containing site-compatible ground motion time-histories whose spectral mean and variability match those obtained from any of the usually employed target spectra used in the earthquake engineering practice. An online tool implementing the proposed methodology is also freely provided.

**KEYWORDS**

artificial accelerograms, ground motion model, non-stationary, spectrum-compatible, stochastic process, variability

## 1 | INTRODUCTION

Response history analysis is widely used for the performance assessment of structural systems under seismic loading. The input earthquake actions are represented by suites of accelerograms that are compatible with a predefined hazard scenario for the site of interest. A common approach for achieving seismic hazard compatibility involves matching the spectral mean of an accelerogram suite to a target acceleration response spectrum. The latter is either a uniform hazard

spectrum (UHS) which typically takes the form of a design spectrum,[1,2] or a conditional mean spectrum (CMS).[2,3] In the field of Probabilistic Seismic Hazard Analysis (PSHA), a UHS provides an envelope of spectral accelerations at all periods with a given exceedance probability. In this respect, UHS correspond to conservative hazard estimates. More recently, the CMS has been recognized as an alternative to the UHS. The CMS provides an improved representation of the hazard at a site because of the realistic correlation between spectral amplitudes at different periods of vibration. Additionally, the CMS offers a less conservative hazard representation. Alternatively, the target spectrum may be obtained from a ground motion model (GMM) corresponding to a specific magnitude-distance scenario and site conditions and containing more detailed hazard information for the site of interest.

The acceleration time-histories adopted for seismic simulations can be either past-recorded (natural) or artificial. Engineers conventionally follow the practice of selecting and scaling suitable past-recorded ground motions from online databases. These accelerograms, however, have been recorded on different locations from the site of interest and thus correspond to different magnitude-distance scenarios and soil characteristics. Furthermore, in many cases, high-resolution hazard analysis may be constrained by the limited availability of ground motions that match the target spectral ordinates. This limitation becomes particularly evident for high limit-states like collapse, where the analysis is restricted by the scarcity of sufficiently strong recorded ground motions. Consequently, a substantial debate has been raised from the selection of a limited number of scaled past-recorded accelerograms. Note in passing that the challenge of selecting and scaling earthquake records still remains a highly controversial issue in the relevant literature.[4,5] As a result, several algorithms that aim to address practically the issue of record selection have been proposed.[3,6,7]

The use of artificial accelerograms is an alternative option that overcomes the problems associated with the selection of natural seismic records. More specifically, artificial accelerograms can be easily generated at the frequency bands of interest while having the desired features using several methods available in the literature. Moreover, seismic codes (e.g., Eurocode 8,[1] ASCE 7[2]) recommend the use of artificial or synthetic ground motions, yet they do not propose a specific method for their generation. In the general case, due to the random nature of the seismic actions, artificial ground motion time-histories can be represented by *stochastic processes*. The available methods range from *source-based models* that follow a seismological approach, to *site-based models* that simulate acceleration time-histories based on a target ground motion record. Furthermore, a large number of *spectrum-based models* that focus on generating artificial accelerograms that are compatible with a target design spectrum have also been proposed in the literature.

Among the aforementioned methods for generating artificial accelerograms, *source-based models* are physics-based simulations that use the stochastic representation of various seismological parameters, mainly the source, travel path, and site effects. In these models, the frequency content of the simulated accelerograms is controlled by the seismologically-modeled source. Two main approaches exist in the literature: the point-source simulation,[8] and the finite-fault simulation.[9] However, source-based models come with a limitation: they require detailed knowledge of the seismological information at the site of interest that is often not available. Moreover, they rely on demanding computations, which renders them impractical for everyday engineering applications. As a result, these models are primarily used for research-oriented objectives.

On the other hand, stochastic earthquake models that are suitable for everyday engineering applications usually comply with site and/or spectrum-dictated requirements. As a result, *site-based models*, *spectrum-based models*, and *hybrid site and spectrum-based models* are typically adopted in practice. Various techniques have been proposed in the literature to generate this kind of models, including the filtered white noise processes,[10] filtered Poisson processes,[11] auto-regressive moving average processes (ARMA),[12] and the widely employed spectral representation models.[13] More recent approaches are based on signal processing operations like the Fourier Transform (FT),[14] the Wavelet Transform,[15] the S-Transform,[16] and the Hilbert-Huang Transform.[17] Furthermore, lately, there has been a growing interest in models capable of generating artificial accelerograms with varying spectral and temporal characteristics.[10,18,19] Finally, it is noted that the aforementioned methods generate single-component ground motions, while few site-based models that focus on generating multi-component ground motions can be found in the literature.[20,21]

The power spectrum is a core model for the representation of the excitation process and is widely applied in the literature due to its easy implementation in the framework of stochastic dynamics approaches. The concept is no longer hindered by the problems that it faced at its early stages back in 1947, when Housner[22] with very limited data available, proposed the white noise model for earthquake representation. In 1976, Vanmarcke[23] concluded that the basis for generating target spectrum-compatible accelerograms relies on the relationship between the values of the *power spectral density (PSD)* function and the response spectral values for a given damping ratio via the *first passage problem*. Since then, various researchers have proposed methods for the determination of a design spectrum-compatible PSD function, for example, Vanmarcke and Gasparini,[24] Cacciola et al.,[25] Kanai-Tajimi,[26,27] Clough-Penzien,[28] and Spanos and Vargas Loli[29] among others.

The generated accelerograms can exhibit different characteristics in terms of stationarity. More specifically, they can be stationary, quasi-stationary (or separable), or fully non-stationary (or non-separable). Stationary ground motions exhibit no amplitude or frequency variation in time, whereas quasi-stationary models are a step further and they achieve only amplitude variation in time while their frequency modulation remains constant. Fully non-stationary (non-separable) models generate ground motions that resemble the nature of real seismic ground motions by possessing a continuously evolving amplitude and frequency content in time. A careful consideration of record non-stationarity is necessary for generating artificial acceleration time-histories that are expected to produce realistic structural responses. Stationary accelerograms may have an excessive number of cycles and, as a result, they may contain much more energy compared to actually recorded ground motions.[30] Furthermore, from a performance based perspective, there is a considerable need for tracing moving resonance phenomena induced from spectral non-stationarity.[31–33] In order to overcome this issue, various methodologies have been proposed for producing non-stationary artificial accelerograms.

Temporal non-stationarity is typically introduced by the modification of a simulated stationary accelerogram with a suitable deterministic time (i.e., amplitude) modulating function, called *modulating function* or *envelope function*. Various shapes of this function have been proposed, that is, exponential,[8] trapezoidal,[34] gamma function[35]; or it can be energy compatible.[36] Fully non-stationary signals may be produced using the power spectrum and more specifically, the *evolutionary power spectral density (EPSD)* function. In this case, the evolving amplitude and spectral content of the accelerogram are modeled using either a time-frequency envelope function that modifies the PSD function of a stationary stochastic process,[37] or signal processing operations like the Wavelet Transform.[38] Alternatively, various techniques have been proposed in the literature in order to model the non-stationary characteristics of the produced accelerograms by borrowing the non-stationary properties of a recorded ground motion.[39,40]

The use of artificial accelerograms for seismic simulations has found many applications in structural engineering. The continuous development and increase of the computational capabilities have established a new framework for the seismic demand and capacity assessment of engineering structures. New approaches in structural analyses tend to go beyond the prescriptive mindset of design codes by incorporating probabilistic models that consider uncertainties and variations in ground motions as well as in structural properties.[41] For example, Monte Carlo Simulation (MCS) techniques emerge as powerful tools for evaluating the reliability of a structural system[42] and require the generation of artificial acceleration time-histories. However, there are cases where the computational cost of these techniques can be prohibitive, therefore, alternative efficient approximate analytical/numerical techniques have been developed. In the field of stochastic dynamics, power spectrum modeling techniques harness the potential of random vibration theory in order to provide efficient techniques for response determination and risk/reliability assessment at a low computational cost.[32,33,43–46] These approaches use artificial accelerograms and they offer a straightforward implementation that relies on the power spectrum.

Alternative to MCS and stochastic dynamics techniques are practice-oriented probabilistic models that consist of conditional, intensity measure (IM) based approaches. These approaches encompass two separate probabilistic steps. More specifically, the first step involves the seismic hazard assessment, which includes the PSHA, or the use of the CMS or GMMs, in order to provide a statistical description of the IM. The second step consists of the evaluation of the seismic demand based on specific values assumed by the IM. The records used in such applications can be past-recorded,[47] however artificially generated suites of ground motions are also often adopted.[48–50] Such analysis methods for structural performance assessment include Incremental Dynamic Analysis (IDA),[51] Cloud analysis, and Multiple-Stripe Analysis (MSA)[47] methods, as well as surrogate modeling[48] approaches. In general, these methods are more appealing to engineering practice, hence the orientation of this work.

The paper presents a practical and computationally efficient probabilistic methodology for the stochastic generation of suites of fully non-stationary artificial accelerograms that are compatible with a target spectral mean and a target variability for the whole period range.[52,53] The proposed model combines the general idea of the record selection procedure proposed by Jayaram et al.[3] with spectral representation techniques for the generation of artificial accelerograms that use a design spectrum-compatible PSD function. More specifically, multiple target response spectra are produced from a random vector that follows the normal distribution and is statistically defined by the target spectral parameters. For every produced target spectrum, a corresponding artificial accelerogram is generated, whose response spectrum matches the assigned individual spectrum. Furthermore, two simple approaches are proposed for producing fully non-stationary artificial accelerograms: the *site and spectrum based variant* and the *evolutionary power spectrum based variant*. The site and spectrum based variant employs a few recorded accelerograms from past earthquake events at the site of interest and uses them as seed records in order to model the non-stationarity. The evolutionary power spectrum based variant employs the power spectrum and a new time-frequency modulating function that is probabilistically modeled using a GMM

that provides the significant duration. In both variants, spectrum compatibility is achieved through the PSD function. This characteristic makes both variants applicable in stochastic dynamics problems. It is worth noting that the proposed methodology is independent of the number of accelerograms contained in the databases and it does not require scaling. Furthermore, it allows to generate as many as required artificial accelerograms for advanced seismic reliability analyses.

The paper aims to offer a tool for practical engineering applications like dynamic structural analysis, or the performance-based assessment of structures. The novel contributions of the proposed work refer to the compatibility of the suite with a target spectral variability, the consideration of spectral correlation at pairs of periods, the variation of the amplitude and frequency modulation features of the accelerograms within a produced suite, and the proposal of a new, probabilistically defined, time-frequency modulating function that is compatible with the strong motion duration of a seismic hazard scenario. Regarding the target spectral variability, it has to be stressed that the majority of the spectrum-based artificial accelerogram generation models that have been proposed in the literature ensure compatibility only with a target mean spectrum, for example refs. [39, 40]. The spectral variability of suites of ground motions, however, affects significantly the structural performance assessment. Therefore, the proposed methodology has the advantage that the produced suites of accelerograms have a controlled target variability for every period value, while also taking into account a correlation structure at different periods of vibration. Furthermore, the proposed approach generates suites of fully non-stationary accelerograms, whereas a relative work by Zentner[19] produces only quasi-stationary accelerograms. Moreover, as the PSD function is directly related to the target spectrum, having a suite that contains accelerograms with different target spectra overcomes, for both variants, the common drawback of producing artificial time-histories with the same spectral features. Another issue in generating suites of ground motions is that the same deterministic procedure is applied for each accelerogram, using one power spectrum and fixed modulating function values. This approach results in ground motions characterized by very similar amplitude and frequency modulation. The proposed methodology, in both of its variants, overcomes this issue. Additionally, compared to relative works,[18] it has the advantage that it ensures that the amplitude and frequency modulation features are compatible with the site of interest. More specifically, the site and spectrum based variant involves the generation of suites of artificial accelerograms by employing and randomly sampling past-recorded seismic accelerograms from the site of interest as initial seed records. Therefore, the produced accelerograms show variation in duration and are compatible with the site's seismicity. The evolutionary power spectrum based variant uses a new, strong motion compatible, time-frequency modulating function. In contrast to popular methods in the literature that use deterministic envelope functions, this new function is modeled probabilistically in terms of strong motion duration variables using a GMM, and a fixed frequency parameter. As a result, the generated accelerograms possess variation in duration, amplitude and frequency modulation, and compatibility with the strong motion duration of the desired seismic scenario. Finally, the proposed methodology aims to offer a practical tool for the everyday needs of engineering practice in a consistent and code-compliant manner. To achieve this goal, it relies on well-established models and empirically confirmed assumptions, avoiding unnecessary complications.

The remainder of this paper is organized as follows: In Section 2 some preliminary concepts regarding the generation of artificial accelerograms are introduced. Next, in Section 3 the proposed methodology is analyzed, step by step, for both of its variants. In Section 4, two illustrative examples are presented in order to display its steps and efficiency, as well as a discussion on the advantages, assumptions, and applications of the proposed methodology is provided. Finally, in Section 5 the drawn conclusions are presented.

## 2 | PRELIMINARY CONCEPTS: THE SPECTRAL REPRESENTATION METHOD

### 2.1 | Spectral representation technique for the stationary case

Target spectrum-compatible stationary accelerograms can be simulated as stochastic processes using spectral representation techniques. Following Shinozuka and Deodatis,[13] the ground motion due to a seismic event can be modeled as a zero-mean stationary Gaussian stochastic process $a_g^s(t)$ of finite duration $T_s$, generated as the superposition of harmonic functions with random phase angles:

$$a_g^s(t) = \sum_{i=1}^{N} \sqrt{2G_s(\omega_i)\Delta\omega}\cos(\omega_i t + \theta_i) \tag{1}$$

where $N$ is the number of harmonics to be superimposed, $\omega_i$ is the angular frequency of the $i^{th}$ harmonic, $\Delta\omega$ is the constant integration step, and $\theta_i$ are the random phase angles, uniformly distributed in the interval $[0, 2\pi]$. Furthermore, the

amplitude of every component is related to the one-sided PSD function $G_s(\omega_i)$ of the stochastic seismic motion. Compatibility with a target spectrum is achieved by the determination of $G_s(\omega_i)$ based on the random vibration analysis approach proposed by Vanmarcke and Gasparini[24] and further developed by Cacciola et al.[25] The basis of the method is the evaluation of a one-sided PSD $G_s(\omega_i)$ which is consistent with a target pseudo-acceleration response spectrum $S_a^*(\omega_i, \zeta)$ of a quiescent elastic single-degree-of-freedom (SDOF) oscillator of undamped angular frequency $\omega_i$ and damping ratio $\zeta$, that is subjected to the generated ground acceleration $a_g^s(t)$. If $X_i(t)$ is the obtained stochastic response process, the pseudo-acceleration response spectrum is:

$$S_a^*(\omega_i, \zeta) = \eta_{X_i} \omega_i^2 \sqrt{\lambda_{0,X_i}} \tag{2}$$

where $\eta_{X_i}$ is the peak factor and $\lambda_{0,X_i}$ is the variance of the stochastic response process $X_i(t)$. The peak factor $\eta_{X_i}$ is the critical factor by which the standard deviation $\sqrt{\lambda_{0,X_i}}$ of the considered elastic oscillator response is multiplied to predict a level of spectral acceleration $S_a^*(\omega_i, \zeta)$ below which the peak response will remain in the interval of $T_s$, with probability $p$.[46] The "$_s$" in $T_s$ and $G_s(\omega_i)$ refers to stationarity. The evaluation of $\eta_{X_i}$ is related to the concept of the first-passage problem. According to the hypothesis of a barrier outcrossing in clumps,[54] the peak factor is obtained as:

$$\eta_{X_i}(T_s, p) = \sqrt{2 \ln \left\{ 2N_{X_i} \left[ 1 - \exp\left( -\delta_{X_i}^{1.2} \sqrt{\pi \ln (2N_{X_i})} \right) \right] \right\}} \tag{3}$$

where $N_{X_i}$ is the mean zero crossing rate and $\delta_{X_i}$ is the spread factor of the stochastic response process $X_i(t)$, defined as:

$$N_{X_i} = \frac{T_s}{2\pi} \sqrt{\frac{\lambda_{2,X_i}}{\lambda_{0,X_i}}} (-\ln p)^{-1} \quad \text{and} \quad \delta_{X_i} = \sqrt{1 - \frac{\lambda_{1,X_i}^2}{\lambda_{0,X_i} \lambda_{2,X_i}}} \tag{4}$$

where $\lambda_{n,X_i}$ is the $n^{th}$ order ($n = 0, 1, 2$) spectral moment of the stochastic response process $X_i(t)$, calculated as:

$$\lambda_{n,X_i} = \int_0^\infty \frac{\omega^n}{(\omega_i^2 - \omega^2)^2 + (2\zeta\omega_i\omega)^2} G_s(\omega) d\omega \tag{5}$$

In order to determine the target spectrum-compatible PSD $G_s(\omega_i)$, it is necessary to evaluate the peak factor and the variance of the SDOF response. However, as observed by Equations (3)–(5), these two parameters depend on the input PSD itself, thus requiring a solution of the inverse stochastic dynamics problem. In this framework, the variance $\lambda_{0,X_i}$ of the response process can be approximated as[23]:

$$\lambda_{0,X_i} = \frac{G_s(\omega_i)}{\omega_i^3} \left( \frac{\pi}{4\zeta} - 1 \right) + \frac{1}{\omega_i^4} \int_0^{\omega_i} G_s(\omega) d\omega \tag{6}$$

Moreover, Cacciola et al.[25] proposed that the mean zero crossing rate and the spread factor are evaluated approximately with reference to a white-noise input[55]:

$$N_{X_i} = \frac{T_s}{2\pi} \omega_i (-\ln p)^{-1} \tag{7a}$$

$$\delta_{X_i} = \sqrt{1 - \frac{1}{1 - \zeta^2} \left( 1 - \frac{2}{\pi} \arctan \frac{\zeta}{\sqrt{1 - \zeta^2}} \right)^2} \tag{7b}$$

Approximating the target PSD with a constant piecewise function, the integral of Equation (6) can be obtained as a discrete summation. Replacing the obtained $\lambda_{0,X_i}$ in Equation (2) leads to the following expression for the spectral acceleration

$S_a^*(\omega_i, \zeta)$:

$$S_a^{*2}(\omega_i, \zeta) = \eta_{X_i}^2 G_s(\omega_i)\omega_i\left(\frac{\pi - 4\zeta}{4\zeta}\right) + \eta_{X_i}^2 \Delta\omega\left(\sum_{k=1}^{i-1} G_s(\omega_k) + G_s(\omega_i)\right) \tag{8}$$

Finally, the target spectrum-compatible one-sided PSD function $G_s(\omega_i)$ of the stationary process can be obtained solving Equation (8) with respect to $G_s(\omega_i)$ as follows:

$$G_s(\omega_i) = \begin{cases} \dfrac{4\zeta}{\omega_i\pi - 4\zeta\omega_{i-1}}\left(\dfrac{S_a^{*2}(\omega_i, \zeta)}{\eta_{X_i}^2} - \Delta\omega\displaystyle\sum_{k=1}^{i-1} G_s(\omega_k)\right), & \omega_i > \omega_0 \\ 0, & \omega_i \le \omega_0 \end{cases} \tag{9}$$

The range of $\omega_i$ is defined in the interval $[\omega_0, \omega_u]$, where $\omega_u$ is an upper cut-off frequency beyond which the PSD function $G_s(\omega_i)$ is assumed to be zero for either mathematical or physical reasons and $\omega_0$ is the lowest frequency bound of the existence domain of Equation (3). For Equation (7) in particular, the value of $\omega_0$ is 0.36 rad/s.[25] This value can not be less than 0.36 rad/s in this case since lesser values make the quantity inside the root in Equation (3) negative. It should be noted that, for $i = 1$, $G_s(\omega_1) = 0$.[13] The accelerograms generated by combining Equations (1) and (9) are stationary and have all the same duration $T_s$.

## 2.2 | Generation of non-stationary ground motions

### 2.2.1 | Modeling the temporal non-stationarity

As discussed in the Introduction, integrating non-stationarity into artificial accelerograms is essential for accurately representing the dynamic and evolving characteristics of seismic events. Temporal (or amplitude) non-stationarity is typically introduced with a *time-modulating function* $\varphi(t)$. The first techniques for generating artificial accelerograms typically were based on time-modulating functions in order to produce quasi-stationary (or separable) accelerograms.[24] However, more recent approaches that generate fully non-stationary (or non-separable) accelerograms, tend to use time-modulating functions for the modeling of the temporal stationarity[8,37,39] as well. As already mentioned in the Introduction, these functions can have various shapes. In this study, the following piece-wise envelope function of Jennings et al. [34] has been adopted:

$$\phi(t) = \begin{cases} \left(\dfrac{t}{t_1}\right)^2, & t < t_1 \\ 1, & t_1 \le t \le t_2 \\ \exp -\dfrac{3}{t_f - t_2}(t - t_2), & t > t_2 \end{cases} \tag{10}$$

The length of the plateau $T_s = t_2 - t_1$ defines the significant (or the strong motion) duration $T_s$ of the accelerogram. The duration of the strong motion is fundamental for engineering applications and should always be compatible with the seismic scenario considered and the soil conditions of the site under study.[56] If $T_s$ is defined as the time interval within which 90% of the energy is dissipated, then $t_1$ and $t_2$ correspond to the time where the 5% and 95% of the total Arias intensity, or energy.

### 2.2.2 | Spectral representation technique for the non-stationary case

Fully non-stationary artificial accelerograms can be generated using a past-recorded accelerogram as a seed record, following the method proposed by Cacciola.[39] Therefore, fully non-stationary and spectrum-compatible accelerograms can be achieved by superimposing the natural record with a corrective term which is a stationary zero-mean Gaussian stochastic

process, multiplied with a time-modulating function $\varphi(t)$:

$$a_g^{ns}(t) = a_{sc}a_R(t) + \varphi(t)\sum_{i=1}^{N}\sqrt{2G(\omega_i)\Delta\omega}\cos(\omega_i t + \theta_i) \tag{11}$$

where $a_R(t)$ is a real recorded accelerogram and $a_{sc}$ is a scaling coefficient:

$$a_{sc} = \min\left[\frac{S_a^*(\omega_i,\zeta)}{S_a^R(\omega_i,\zeta)}\right], \quad i = 1,2,\dots,N. \tag{12}$$

where $S_a^*(\omega_i,\zeta)$ is the target spectral acceleration and $S_a^R(\omega_i,\zeta)$ is the recorded accelerogram's spectral acceleration at frequency $\omega_i$, and $a_{sc} = \max[a_{sc},1]$ for the method to be valid.[39] Spectrum compatibility is achieved through the one-sided PSD function of the quasi-stationary zero-mean Gaussian stochastic process:

$$G(\omega_i) = \begin{cases} \dfrac{4\zeta}{\omega_i\pi - 4\zeta\omega_{i-1}}U\left[\dfrac{S_a^{*2}(\omega_i,\zeta) - (a_{sc}S_a^R(\omega_i,\zeta))^2}{\eta_{X_i}^2} - \Delta\omega\sum_{k=1}^{i-1}G(\omega_k)\right]\times \\ \times\left[\dfrac{S_a^{*2}(\omega_i,\zeta) - (a_{sc}S_a^R(\omega_i,\zeta))^2}{\eta_{X_i}^2} - \Delta\omega\sum_{k=1}^{i-1}G(\omega_k)\right], & \omega_i > \omega_0 \\ 0, & \omega_i \le \omega_0 \end{cases} \tag{13}$$

where $U[\cdot]$ is the unit step function that is used to avoid negative solutions.

### 2.2.3 | Spectral representation technique for the non-stationary and non-separable case

Fully non-stationary artificial accelerograms using an EPSD function can be generated following the method proposed by Preumont.[37] In this method, the EPSD function is determined by equating, for each frequency, the energy of the separable (i.e., quasi-stationary) process with the energy of a non-separable (i.e., fully non-stationary) process. Therefore, the ground motions are generated as:

$$a_g^{ns}(t) = \sum_{i=1}^{N}\sqrt{2G(\omega_i,t)\Delta\omega}\cos(\omega_i t + \theta_i) \tag{14}$$

where in this case, the one-sided EPSD time-frequency function $G(\omega_i,t)$ is defined as:

$$G(\omega_i,t) = G_s(\omega_i)|\Phi(\omega_i,t)|^2\frac{\int_0^\infty\varphi^2(t)\,\mathrm{dt}}{\int_0^\infty|\Phi(\omega_i,t)|^2\,\mathrm{dt}} \tag{15}$$

where $|\Phi(\omega_i,t)|$ is a time-frequency envelope function that performs the time and frequency modulation of the generated accelerogram in order to simulate the characteristic behavior of real recorded accelerograms. More information for this modulating function will be provided in Section 3.2.2.

## 3 | PROPOSED METHODOLOGY

This study proposes a practical probabilistic method for the stochastic generation of suites of fully non-stationary artificial accelerograms that are compatible with a target spectral mean and a target variability in order to achieve seismic-hazard consistency. Once the mean target spectrum and variability are available, an ensemble of target response spectra of specified damping ratio $\zeta$ is produced. Then, for every target spectrum, a corresponding artificial acceleration time-history whose response spectrum matches the particular spectrum is generated. The simulated ground motions are fully non-stationary, distinct, site-compatible, and generated using spectral representation techniques. For a seismic hazard scenario

($M_w$–$R$) and soil conditions, the target mean response spectrum at a specified range of periods $T_i = 2\pi/\omega_i$ can be obtained, either in the form of a UHS, or from a GMM. Variability is typically defined in the case of a GMM, as they provide the mean and standard deviation of the logarithmic spectral acceleration values. In the case of a UHS, it already accounts for variability in spectral accelerations at every period. Jayaram et al.[3] mention that no further variability should be applied to the UHS, "since varying the spectral values is equivalent to varying the associated exceedance rate of the spectral accelerations from period to period".

The proposed methodology includes two distinct variants: the *site and spectrum based variant* and the *evolutionary spectrum based variant*. The former is applicable in cases where regulations impose the use of real recorded acceleration time-histories in the process of generating artificial accelerograms, or simply when there is a need for additional acceleration time-histories due to a limited number of past records from the site of interest. The latter variant is more general in scope and applies to a broad range of problems, from dynamic analyses to stochastic dynamics applications. The first variant of the proposed methodology creates suites of artificial accelerograms using past-recorded seismic accelerograms as seed records in order to model the amplitude and the frequency modulation in time. A small number of records is obtained from the site of interest from past seismic activity and then it is randomly sampled. The second variant uses an appropriate one-sided EPSD function $G(\omega, t)$ which is modeled by a time-frequency modulating function $|\Phi(\omega_i, t)|^2$.

Both variants of the proposed methodology use a different approach for the record duration modeling, and thus avoid creating suites that contain very similar accelerograms of the same duration. The site and spectrum based variant determines the values of $t_1$ and $t_2$ for the time-modulating function $\phi(t)$ from the Husid function of the recorded accelerogram. The evolutionary spectrum based variant defines those values statistically; $t_1$ is randomly sampled from a given interval, and the significant duration $T_s$ is also sampled once the logarithmic mean and standard deviation are known from a GMM. In this variant, a new time-frequency modulating function is proposed, which ensures that the peak of the envelope is compatible with the strong motion duration $T_s$.

The generation of artificial accelerograms typically requires corrective iterations in the frequency domain in order to achieve enhanced spectrum compatibility, for example, the widely applied methods proposed by Vanmarcke and Gasparini,[24] Spanos and Vargas-Loli,[29] and Cacciola.[39] Especially when the proposed methodology is adopted, introducing the target variability increases the method's sensitivity to the individual spectrum matching quality, that is, poor spectrum matching adds spurious variability in the model. The proposed iteration scheme uses the FT instead of the customarily employed PSD function, as it is computationally efficient and capable of achieving the appropriate matching for the objectives of the study. Due to the enhanced spectrum matching, the proposed method is efficient even for a small number of generated accelerograms, for example, seven. The outcome of the proposed methodology is a suite of fully non-stationary ground motion time-histories whose mean and variability match those of a GMM or a code-based design spectrum. The steps are discussed below and are also shown in the flowchart of Figure 1. The online tool for the proposed methodology is freely available at: https://github.com/HeraYanni/ProbGenArtifAccel.git.

## 3.1 | Generation of target spectra

An ensemble of target spectra $S_a^{*j}(T_i, \zeta)$ is produced, with the targeted mean and variability. For this purpose, variability is quantified with the variable $\beta^*(T_i, \zeta)$, and $S_a^{*j}(T_i, \zeta)$ are generated according to the process that follows. The target logarithmic spectral accelerations $\ln\left[S_a^{*j}(T_i, \zeta)\right]$ at every period $T_i$ are sampled as a normally distributed (Gaussian) random variable with mean $\ln[S_a^*(T_i, \zeta)]$ and standard deviation $\sigma^*_{\ln(S_a)}(T_i, \zeta)$:

$$\ln\left[{S_a}^{*j}(T_i, \zeta)\right] = \ln[S_a^*(T_i, \zeta)] + a_j \sigma^*_{\ln(S_a)}(T_i, \zeta) \tag{16}$$

where $a_j$ is a standard Gaussian random variable. This assumption relies on the empirically verified observation that the logarithmic spectral accelerations $\ln\left[{S_a}^{*j}(T_i, \zeta)\right]$ follow the normal distribution, characterized by the mean value and standard deviation.[3] It is noted that Equation (16) assumes perfect positive correlation between pairs of periods, $\rho(T_i, T_{i+1}) = 1$, which is a common assumption. When a GMM is used, the target mean $S_a^*(T_i, \zeta)$ in Equation (16) is the mean spectral value obtained from the GMM at every period $T_i$. In this case, the variability around the target spectrum is determined as the standard deviation of the natural logarithms of the spectral values given from the GMM, that is,

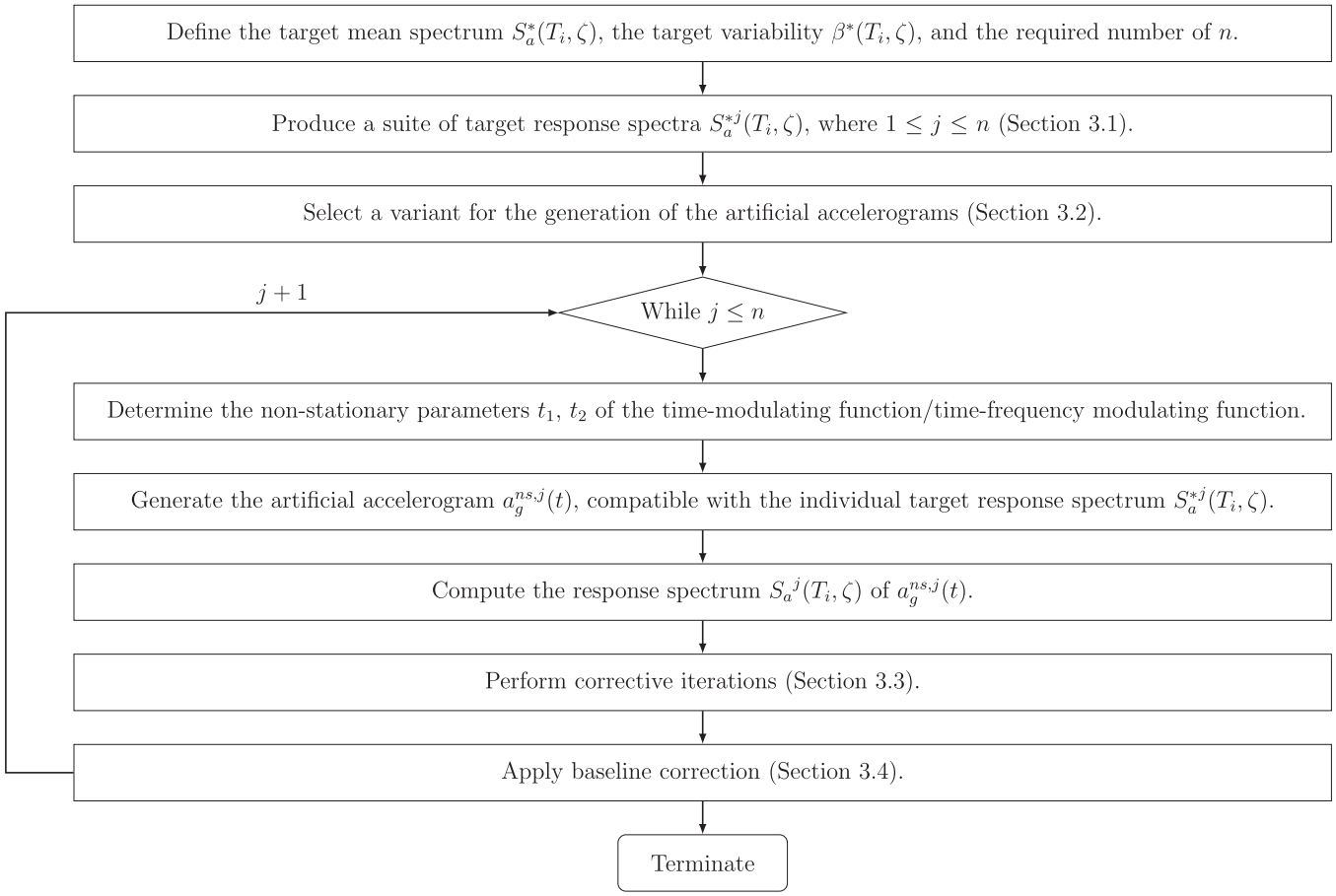


**FIGURE 1** Flowchart of the proposed procedure for generating suites of fully non-stationary artificial accelerograms compatible with a target spectral mean and variability.

$\beta^*(T_i,\zeta) = \sigma^*_{\ln(S_a)}(T_i,\zeta)$. For a suite containing $n$ accelerograms, Equation (16) can be re-written as:

$$S_a^{*j}(T_i,\zeta) = S_a^*(T_i,\zeta)\exp\left[a_j\beta^*(T_i,\zeta)\right] \tag{17}$$

where $1 \le j \le n$. Since perfect positive correlation between pairs of periods has been assumed, the value of the parameter $a_j$ is the same for every period $T_i$ of each record; thus only one value of $a_j$ is needed for every record. Consequently, $a_j$ is generated as a random vector $\boldsymbol{a_n} = [a_1, a_2, \dots, a_n]$ whose elements are standard normal variables. Since the $n$ set of data (number of records) is relatively small, noise is expected on the elements of $\boldsymbol{a_n}$. This sometimes results in significant deviations of the mean $\mu_a$ and the standard deviation $\sigma_a$ of the vector $\boldsymbol{a_n}$ from the expected target statistical values ($\mu_a = 0$ and $\sigma_a = 1$), especially when the number of records is small, for example, $n = 7$. Thus, each element of $\boldsymbol{a}_n$ is "corrected" as follows:

$$a_j = \frac{a_j - \mu_a}{\sigma_a} \tag{18}$$

where $\mu_a$ and $\sigma_a$ are the actual mean and standard deviation in the presence of noise.

In order to generalize the proposed model, Equation (16) is further developed in order to incorporate the target variability in the case where a smooth code spectrum is used. Therefore, the code spectrum's spectral values are considered as the target mean $S_a^*(T_i,\zeta)$ and the variability, in this case, is more easily defined by specifying a constant Coefficient of Variation (CoV) value for all periods, thus $\beta^*(T_i,\zeta) = CoV$. Equation (16) is again adopted, but without the logarithms, as follows:

$$S_a^{*j}(T_i,\zeta) = S_a^*(T_i,\zeta) + a_j\sigma^*_{S_a}(T_i,\zeta) \tag{19}$$

where $\sigma^*_{S_a}(T_i,\zeta) = \beta^*(T_i,\zeta)S^*_a(T_i,\zeta)$. In order to ensure that every individual target spectrum $S^{*j}_a(T_i,\zeta)$ does not receive negative values, the value of $[1 + a_j\beta^*(T_i,\zeta)]$ must be greater than zero. This results in the following limit for the values of $a_j$:

$$a_j > -\frac{1}{\beta^*(T_i,\zeta)} \tag{20}$$

The limit is applied when generating the random values $a_j$. If Equation (20) is not satisfied for all records, then a new set of random values $a_j$ is produced until the limit is satisfied.

The correlation structure for spectral accelerations at different periods of vibration is an important feature when considering ground motions for the analysis of multi-degree of freedom systems (MDOFs). Following Tarbali and Bradley,[57] Equation (16) is extended in order to account for the correlation between spectral values:

$$\ln\left[{S_a}^{*j}(T_i,\zeta)\right] = \ln\left[S^*_a(T_i,\zeta)\right] + a_{ij}\sigma^*_{\ln(S_a)}(T_i,\zeta) \tag{21}$$

where $1 \le i \le N$, and $N$ is the number of period values considered. Since different correlation values between pairs of periods have been assumed, in this case, the value of the parameter $a_{ij}$ is different for every period $T_i$ of each record; thus different values of $a_{ij}$ are needed for all the periods of every record. Consequently, $\boldsymbol{a_n}$ is generated as a $N \times n$ matrix that follows a standard multivariate normal distribution, and each element $a_{ij}$ belongs to the $i^{th}$ period of the $j^{th}$ record, where $i \in [1,N]$ and $j \in [1,n]$.

The correlation between spectral accelerations at pairs of periods is expressed through the $N \times N$ correlation matrix $\boldsymbol{\rho_{ln}}$, which can be obtained from empirical correlation models, such as that of Baker and Jayaram.[58] The correlated random realisations of $a_{ij}$ that follow the standard normal distribution for the $j^{th}$ record are generated as:

$$\boldsymbol{a_j} = \boldsymbol{0} + \boldsymbol{Lz} \tag{22}$$

where $\boldsymbol{a_j}$ is the $j^{th}$ column of the $\boldsymbol{a_n}$ matrix, and $\boldsymbol{z}$ is a vector of uncorrelated random variables that follow the standard Gaussian distribution. The matrix $\boldsymbol{L}$ is obtained from the Cholesky decomposition of the correlation matrix (since the standard deviation of the distribution is 1) as $\boldsymbol{\rho_{ln}} = \boldsymbol{LL}^T$. This procedure generates the $j^{th}$ column of the $\boldsymbol{a_n}$ matrix.

The rows of the $\boldsymbol{a_n}$ matrix should follow the standard normal distribution as well, so that the logarithmic spectral accelerations $\ln\left[{S_a}^{*j}(T_i,\zeta)\right]$ would follow the normal distribution. Regarding the implementation of the above model, noise in data is again expected, especially at the distributions of the rows of the $\boldsymbol{a_n}$ matrix, when the number of records is relatively small. Therefore, a MCS procedure is followed for the determination of the $\boldsymbol{a_n}$ matrix, in order to select the best matrix where the mean of every row $\mu_{a,row}$, the standard deviation $\sigma_{a,row}$, and the skewness $k_{a,row}$ ideally are equal to 0, 1, and 0 respectively. Specifically, $\boldsymbol{a_n}$ is generated for a number of trials $n_{trials}$, and for each trial, the matrix is scored based on the summed mean of the squared errors of the rows. Then, the matrix with the best score is selected for the generation of the target spectra. The score is estimated as the weighted sum (over all $N$ rows) of the squared errors of the deviations of the generated parameters from the target distribution parameters:

$$score = \sum_{i=1}^{N}\left[w_1(\mu_{a,row})^2 + w_2(\sigma_{a,row}-1)^2 + w_3(k_{a,row})^2\right] \tag{23}$$

where $w_1, w_2, w_3$ are user-defined weights that control the relative importance of the deviance of the mean, the standard deviation, and the skewness from the desired targets, on the score of each sample matrix. In practice, equal weights can be assumed for the mean and the standard deviation and zero for the skewness.

## 3.2 | Generation of suites of non-stationary ground motions

Two different variants of the proposed methodology are provided for creating suites of fully non-stationary, site and spectrum-compatible accelerograms that posses distinct temporal and spectral non-stationary characteristics: (i) the site and spectrum based variant, and (ii) the evolutionary spectrum based variant.

### 3.2.1 | The site and spectrum based variant

The *site and spectrum based variant* uses past-recorded earthquake ground motions as seed records in order to model the non-stationary characteristics. These seed records consist of recorded accelerograms obtained from the same site, that is, the site of interest, but from different earthquake events. Alternatively, they may be obtained from a site with similar characteristics, such as fault type, soil type, $M_w$–$R$, etc. Therefore, these accelerograms can be retrieved from a ground motion database like the Engineering Strong Motion (ESM)[59] or the Pacific Earthquake Engineering Centre (PEER)[60] database. Naturally, the number of available seed records from the site of interest is typically less than the required for a comprehensive dynamic assessment. In such cases, it is appropriate to produce additional ground motions using samples from the available dataset[50]. Furthermore, this approach is quite useful when regulatory requirements mandate using natural records for the modeling of artificial accelerograms. For example, RG 1.208 US-NRC 2007[61] states that "synthetic motions that are not based on seed recorded time-histories should not be used".

The proposed methodology works as follows: let $k$ historical records be available for the particular site of interest, while a suite of $n$ records is desired, where $k < n$, say $k = 3$ and $n = 20$. The generation of $n$ accelerograms is performed by randomly selecting a record from the $k$ available records and using it as a seed to model the non-stationarity. Note that the selection is random (follows the *uniform* distribution) and hence there is no need for a more elaborate probabilistic procedure. This is due to the fact that the only information extracted from each record are the non-stationary characteristics (i.e., amplitude and frequency modulation) rather than IMs like the amplitude, or the frequency content. The artificial accelerograms are generated using Equations (10)–(13), where $t_1$ and $T_s$ are obtained from the Husid function of the seed accelerogram. The produced suite contains fully non-stationary, spectrum-compatible accelerograms that are consistent with the site's seismicity.

### 3.2.2 | The evolutionary spectrum based variant

The *evolutionary spectrum based variant* generates artificial accelerograms using Equations (14)–(15). In this case, the generation of the accelerograms relies on the power spectrum as well as a new time-frequency modulating function $|\Phi(\omega_i, t)|$. In the context of the modeling of an IM-related modulating function, $|\Phi(\omega_i, t)|$ is defined from the beginning of the strong motion phase $t_1$, the significant duration $T_s$, and a parameter for frequency modulation. More specifically, the time-frequency modulating function $|\Phi(\omega_i, t)|$ has the form below:

$$|\Phi(\omega_i, t)|^2 = t^2 \exp\left[-(p_0 + p_1\omega_i)t\right] \tag{24}$$

where $p_0$ and $p_1$ are parameters that model the temporal and the spectral non-stationarity, respectively. This form ensures that the amplitude and the frequency evolution with time of the generated acceleration time histories will resemble that of recorded ground motions. Specifically, the exponential form ensures that the amplitude of the generated signal will gradually increase from zero to achieve a nearly constant peak, then gradually decay to zero. Furthermore, this form also ensures that the high-frequency components will have a significant influence at the initial stages of the acceleration time-history, gradually diminishing as time progresses, leading to a motion that is dominated by low-frequency components as it decays. This approach is in accordance with real seismic records, where typically the initial seconds of the motion are dominated by high-frequency P waves, succeeded by moderate-frequency S waves—which dominate the strong-motion phase-, and as the shaking progresses, low-frequency surface waves tend to dominate the motion.

Aiming to model an IM-related modulating function, the parameter $p_0$ is directly related to the significant duration IM. Specifically, $p_0$ is obtained from the local maximum of the function in the time axis, resulting to $p_0 = 2/t_0$, where $t_0$ is the time instant when the maximum of $|\Phi(\omega_i, t)|$ appears. The parameter $t_0$ is set as $t_0 = t_1 + T_s/2$ so that the peak of the envelope function is always compatible with the strong motion duration $T_s$. After several calibration tests, realistic frequency modulation is ensured by setting $p_1 = 0.01$. Therefore, the proposed time-frequency modulating function results to:

$$|\Phi(\omega_i, t)|^2 = t^2 \exp\left[-\left(\frac{2}{t_1 + T_s/2} + 0.01\omega_i\right)t\right] \tag{25}$$

The varying parameter $2/(t_1 + T_s/2)$ inside the exponential defines the amplitude modulation characteristics of the function, whereas the frequency modulation is ensured by the $0.01\omega_i$ part. Since the modulating function is part of a spectrum-compatible accelerogram generation methodology, no parameter to control the amplitude value was defined. For a non-separable process, the decay of the time-frequency modulating function, and thus of the accelerogram amplitude, depends on $t_1$, $T_s$, and the frequency modulation part. It is noted that the decay is defined by the constantly increasing negative value inside the exponential of Equation (25).

The total duration of the signal is modeled by taking into account the typical durations of ground motions, which generally fall within the range of 20–60 s.[10] Additionally, it's important to ensure that a sufficient interval $t_r$ is provided for the function to achieve zero residuals on the time-axis. Therefore upon obtaining $T_s$, the remaining time after $t_1 + T_s$ should be enough to include the gradual attenuation of the accelerogram's amplitude back to the baseline. Thus, the total duration $t_f$ of the generated signal is:

$$t_f = t_1 + T_s + t_r \tag{26}$$

The parameters of Equation (26) are user-defined and can be freely adjusted. In the proposed methodology, the beginning of the strong motion phase $t_1$ is uniformly sampled within the interval 3 to 5 s, while the duration $T_s$ is obtained from a strong motion GMM that is consistent with the characteristics of the site of interest. An interval of $t_r = 30\,s$ was found adequate for the applications examined.

The exact values of $t_1$ may range from fractions of a second to several seconds after the beginning of the earthquake. This instant is scenario-dependent and is typically a function of source, wave propagation, and site conditions. For example, observation points located furthest from the source will have a strong motion phase that starts later compared to that of observation points close to the source. For moderate to strong seismic events, the strong motion phase typically starts within a few seconds after the earthquake begins. The choice of the interval of 3 to 5 s in the proposed methodology for the sampling of $t_1$ is based on the assumption of point-source modeling.[8] Thus, the zero time point of the generated signal does not coincide with the earthquake initiation at the source. It is noted that, in the proposed methodology, the beginning of the strong motion phase $t_1$ is a user-defined parameter that can be appropriately adjusted given a higher volume of information is available. Different approaches can also be adopted, like the definition of a 1 to 5 s interval by Zentner,[19] or by dividing the focal distance $R_{hypo}$ in kilometers by a factor defined by the P and S wave propagation velocities $V_pV_s/(V_p - V_s)$, as in the work of Sabetta et al.[16]

The duration of the strong motion phase $T_s$ is obtained from a GMM that is consistent with the characteristics of the site of interest. $T_s$ is defined as a random variable that follows the log-normal distribution. This assumption is based on empirically verified observations that ground motion IMs can be modeled as random variables that follow the log-normal distribution.[62] GMMs provide the mean of natural logarithm, that is, $\ln T_s$, and the standard deviation $\sigma_{ln,Ts}$. The proposed methodology focuses mainly on response spectrum mean and variability matching, and single $M - R$ scenarios. In this context, the main difficulty lies in the scarcity of GMM models that provide both the spectral ordinates and the strong motion duration $T_s$. In the absence of such information, different GMMs from a similar seismotectonic environment can be borrowed. Instead, a holistic approach like the Generalized Conditional Intensity Measure (GCIM)[62] can alternatively be adopted. According to the GCIM, a joint multi-variate distribution of IMs is produced and is used as the target. The proposed methodology can be extended for this case by following the procedure of Tarbali and Bradley[57] for the generation of random realizations of correlated IMs.

Figure 2 shows the proposed time-frequency modulating function side-by-side to that of a real earthquake ground motion. The time-frequency plots show the modulus of the continuous wavelet transform (CWT) of the signals. The values of $t_1$, $T_s$, and $t_f$ of the modulating function are that of the corresponding ground motion record. It can be observed that the modulating function captures the nature of recorded ground motions in terms of amplitude and frequency modulation in time. Moreover, for demonstration purposes, a pertinent case is shown in Figure 3, where the time-frequency modulating function is plotted for specific values of $t_1 = 3$s and $T_s = 10$s. It is observed that, the peak of the function is compatible with the strong motion duration $T_s$: the peak occurs at $t_{0,a} = 3s + 10s/2 = 8s$.

The outcome of the *evolutionary spectrum based variant* is a suite of ground motions that contains fully non-stationary, spectrum-compatible accelerograms that are consistent with a site-specific, predefined seismic hazard scenario.

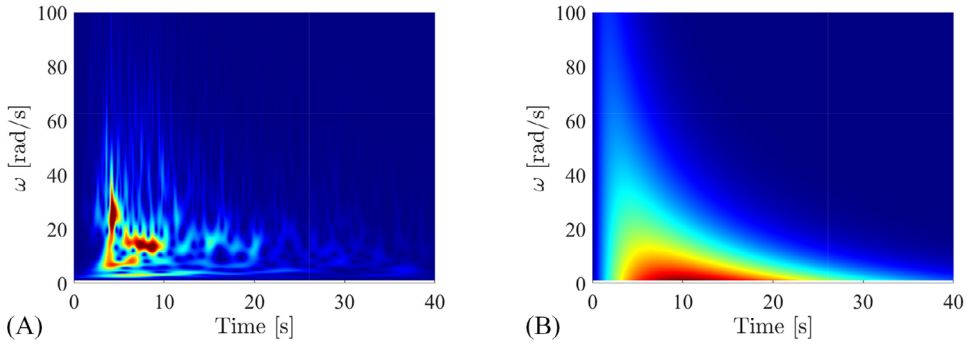


**FIGURE 2** Assessment of the proposed time-frequency modulating: (A) CWT modulus of the seismic record Corinth Greece, 2/24/1981 (component T), (B) the proposed time-frequency modulating function for $t_1 = 3.78$ s, $T_s = 13.94$, and $t_f = 40.93$ s. CWT, Continuous Wavelet Transform.

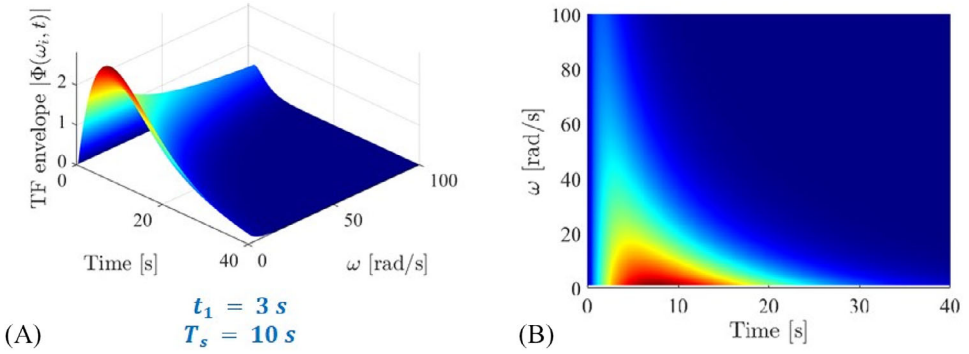


**FIGURE 3** The time-frequency modulating function $|\Phi(\omega_i, t)|$ using Equation (25) for $t_1 = 3$ s and $T_s = 10$ s.

## 3.3 | Enhanced matching iterative scheme

Artificial accelerogram generation methods usually require corrective iterations in the frequency domain in order to enhance the matching between the generated accelerogram's spectrum and the target spectrum. Most methods in the literature modify iteratively the PSD function as follows:

$$G(\omega_i)^{(k+1)} = G(\omega_i)^{(k)} \left[ \frac{S_a^*(\omega_i, \zeta)}{S_a^{(k)}(\omega_i, \zeta)} \right]^2 \tag{27}$$

where $S_a^*(\omega_i, \zeta)$ is the target spectrum and $S_a^{(k)}(\omega_i, \zeta)$ is mean response spectrum the generated accelerograms determined at the $k^{th}$ iteration. If, after a number of iterations, the convergence cannot be achieved for a preselected threshold, a new accelerogram is generated and the procedure is repeated. This method however may require increased computational time until an acceptable accelerogram is obtained. Additionally, if the target error value is very small, it is possible that the criteria cannot be met at all.

Poor spectrum matching in the proposed algorithm results in significant differences between the achieved $\beta(T_i, \zeta)$ and the target $\beta^*(T_i, \zeta)$ variability. In general, there are methods that target on compatible power spectra to be used in conjunction with stochastic dynamics tools. The proposed methods herein are oriented toward studies of the MCS kind. Therefore, in order to improve the control of the variability of the model, the corrective iterations are carried out using the FT, as discussed by Spanos and Vargas Loli[29] and Ferreira et al.[40] This approach was proven more efficient, both computationally and also in terms of spectrum matching. The corrective iterations are carried out for every generated accelerogram individually, as follows:

$$\left| F(\omega_i)^{(k+1)} \right| = \left| F(\omega_i)^{(k)} \right| \left[ \frac{S_a^{*j}(\omega_i, \zeta)}{S_a{}^{j,(k)}(\omega_i, \zeta)} \right] \tag{28}$$

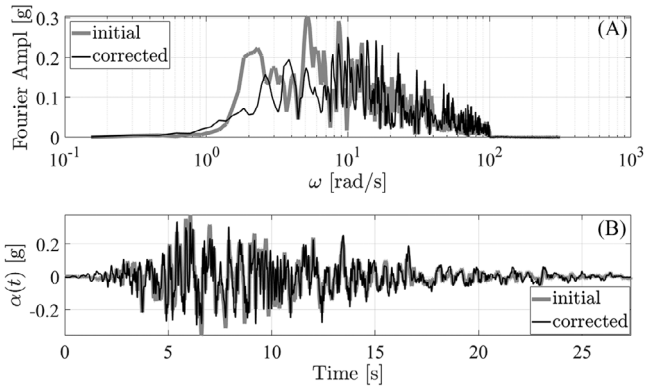


**FIGURE 4** (A) Comparison of the amplitude of the Fourier Transform of a generated accelerogram before and after the corrective iterations. (B) Comparison of a generated accelerogram before and after the corrective iterations.

and

$$\arg\left[F(\omega_i)^{(k+1)}\right] = \arg\left[F(\omega_i)^{(k)}\right] \tag{29}$$

where $F(\omega_i)^{(k)}$ is the FT of the generated accelerogram at the $k^{th}$ iteration, $S_a^{*j}(\omega_i, \zeta)$ is the $j$ target spectrum, and ${S_a}^{j,(k)}(\omega_i, \zeta)$ is the $j$ generated accelerogram's response spectrum determined at the $k^{th}$ iteration. Then, by applying the inverse FT, a new time-history $a_{G_j}^{(k+1)}(t)$ is determined, along with its response spectrum ${S_a}^{j,(k+1)}(\omega_i, \zeta)$. The iteration scheme provided by Equations (28) and (29) modifies the spectral amplitude characteristics of the generated accelerogram, see Figure 4A as well as the amplitude in the temporal non-stationarity, as shown in Figure 4B.

### 3.4 | Baseline correction

After the generation of the seismic accelerograms, the velocity, and subsequently the displacement, time-histories can be obtained through numerical integration. However, for some of the simulated accelerograms, this can result in velocity and displacement trajectories that exhibit an unrealistic baseline drift. This is a baseline correction problem, which can be addressed in the same way as for real recorded accelerograms.[63] In this work, a simple quadratic curve is adopted for the baseline correction in order to yield realistic velocity and displacement time-histories.

## 4 | NUMERICAL EXAMPLES

Two case studies are presented in order to demonstrate the efficiency of the proposed probabilistic generation methodology. The first example considers a target code-based uniform hazard design spectrum and examines the various parameters that define the proposed model. The artificial, fully non-stationary accelerograms are generated following the site and spectrum based variant. In the second example, the artificial and hazard-consistent accelerograms are generated compatible with a seismic hazard scenario that is provided by the BSSA14 model proposed by Boore et al.[64] In this case, non-stationarity is simulated using the evolutionary spectrum based variant.

The choice of the number of corrective iterations depends on various parameters like the desired error level, the shape of the target spectrum and target variability, the ground motion generation methodology, the number of generated ground motions, and the correlation structure between periods. Therefore, in all examples considered, practically 5–10 iterations were found adequate for achieving convergence. In any case, it is a user-defined parameter. The matching quality between the target spectral ordinates and those of the spectra of the generated ground motions can be obtained using the mean square error (MSE), as it ensures an overall evaluation of matching quality across all periods and mitigates the impact of outliers.

**TABLE 1** Suite of real recorded accelerograms used as seed records.

| Event ID | Station name | Component | Date |
|---|---|---|---|
| GR-1999-0001 | SGMA | HN3 | 07-09-1999 |
| EMSC-20180115_000008 | ATH5 | HNN | 15-01-2018 |
| EMSC-20190728_0000106 | ATH5 | HNN | 28-07-2019 |

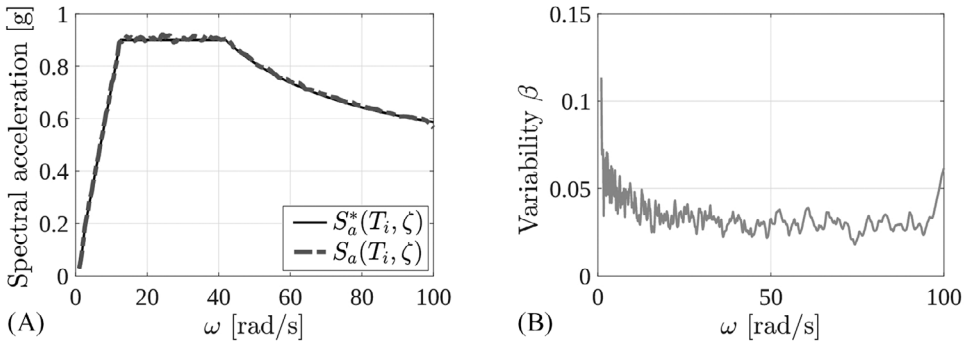


**FIGURE 5** (A) Comparison between the target response spectrum $S_a^*(T_i,\zeta)$ (EC8 design spectrum) and the mean spectrum of the generated accelerograms $S_a(T_i,\zeta)$ with the site and spectrum based variant, (B) the inherent variability $\beta(T_i,\zeta)$ = CoV obtained from the analysis.

## 4.1 | First example: Artificial accelerograms generated by the site and spectrum based variant matching a design code spectrum

A suite of 30 accelerograms is generated following Equations (11)–(13), where only the mean of the suite is matched to the elastic spectrum of Eurocode 8.[1] The parameters assumed for the mean target spectrum $S_a^*(T_i,\zeta)$ are: $a_g = 0.30g$, soil category "B" ($S = 1.20$, $T_B = 0.15$s, $T_C = 0.50$s, $T_D = 2.50$s), damping ratio $\zeta = 5\%$ and importance factor $\gamma_I = 1.00$.

The artificial fully non-stationary accelerograms are generated using the site and spectrum based variant discussed in Section 3.2.1. The frequency range is set $[\omega_0, \omega_u]$ where $\omega_0 = 1$ rad/s and $\omega_u = 100$ rad/s. The number of harmonics to be superimposed is $N = 1000$, which leads to frequency domain integration step $\Delta\omega = 0.1$ rad/s. The number of corrective iterations is set to $n_{iter} = 10$. The site considered is the center of Athens, Greece, where three recorded ground motions are selected in order to model the non-stationarity. The recorded ground motions (Table 1) have been downloaded from the ESM[59] database. The selected accelerograms correspond to different earthquake events, and hence only their time-frequency modulation is required.

After generating the artificial accelerograms, their mean spectrum and CoV are computed and compared with the target spectrum. The results are presented in Figure 5, where Figure 5A shows the mean spectrum matching and 5B shows the variability $\beta(T_i,\zeta)$ (CoV) of the obtained artificial records. As it is observed, there is a perfect match of the mean spectra, whereas the model has a small inherent variability, due to the random phase angles of Equation (11).

In order to further elaborate on the proposed method, the example is extended by introducing target variability in the model. Therefore, the spectral values of the same EC8 spectrum are considered as the target mean $S_a^*(T_i,\zeta)$ and the variability is defined by specifying a constant value of $\beta^*(T_i,\zeta) = CoV = 0.30$ for all periods. A suite of 30 target spectra is generated following Equations (19) and (20), for $n = 30$ and are shown in Figure 6. The remaining problem parameters are the same as before.

The results for the suite of the generated accelerograms are shown in Figure 7. As it is observed, the simulated values are very close to the target ones for both the target spectral mean (see Figure 7A) and the target variability (see Figure 7B), thus proving the efficiency of the algorithm. For the sake of completeness, Figure 7B also shows the inherent variability due to the random phase angles of Equation (11), obtained by matching the suite's mean only to the target spectrum. This variability is less than 5% and does not affect the obtained $\beta(T_i,\zeta)$ when introducing target variability in the model. Examples of three generated artificial accelerograms are shown in Figure 8.

To further examine the effect of spectrum matching on the performance of the proposed method, two suites of 30 artificial accelerograms are generated, one where the corrective iterations are carried out with the PSD function (Equation 27), and another following the FT approach (Equations 28 and 29). In the first case, for every individual target spectrum

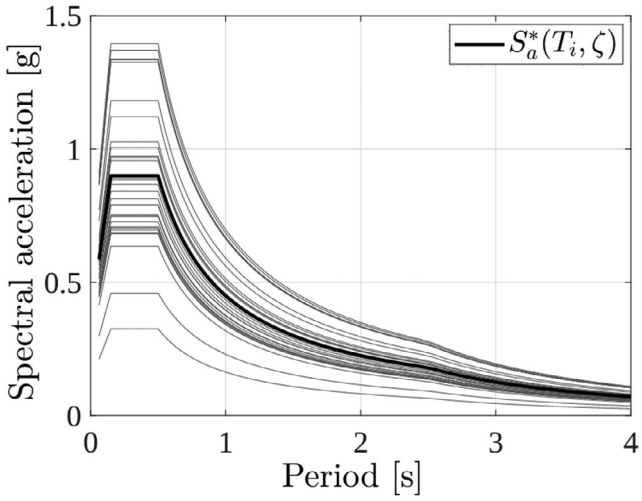


**FIGURE 6** Individual target response spectra $S_a^{*j}(T_i,\zeta)$ probabilistically produced for the generation of 30 artificial accelerograms following Equations (19) and (20) and their respective mean spectrum $S_a^*(T_i,\zeta)$.

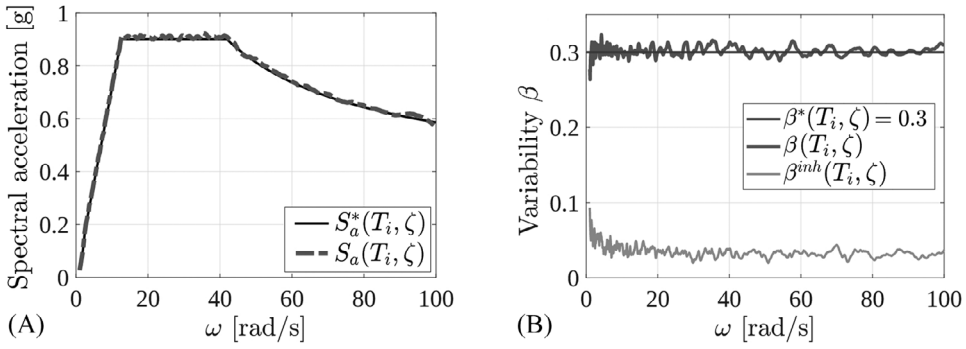


**FIGURE 7** (A) Comparison between the target mean response spectrum $S_a^*(T_i,\zeta)$ (EC8 design spectrum) and the mean spectrum of the generated accelerograms $S_a(T_i,\zeta)$ from the spectra of Figure 6 with the site and spectrum based variant, (B) comparison between the target CoV $\beta^*(T_i,\zeta)=0.30$ and the obtained CoV. CoV, Coefficient of Variation.

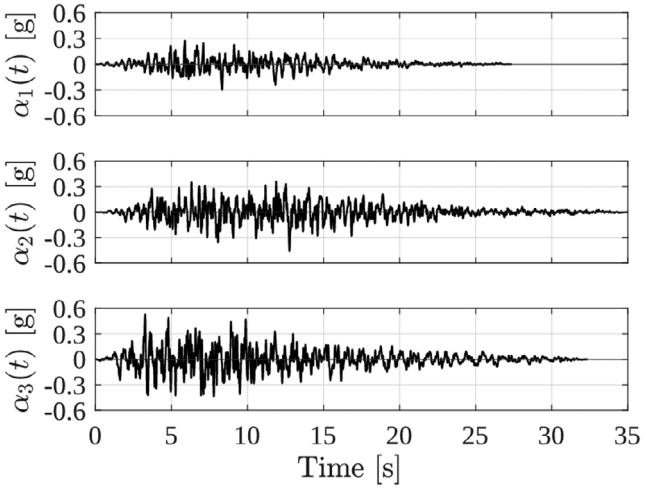


**FIGURE 8** Results of the first numerical example: Three randomly generated accelerograms belonging to the suite produced with the target spectra of Figure 6 and the site and spectrum based variant.

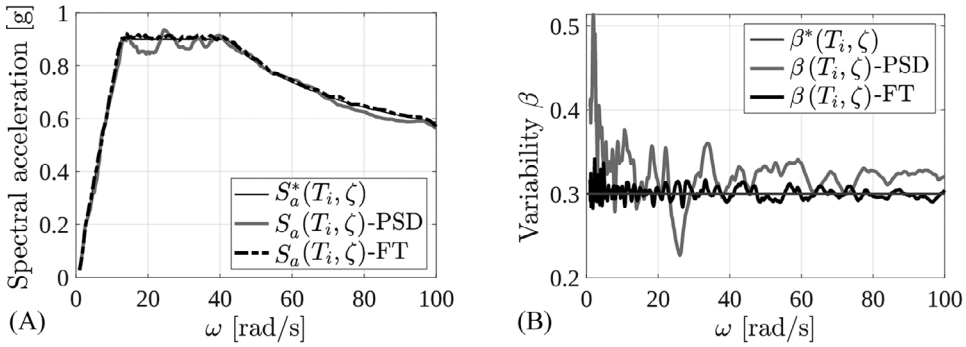


**FIGURE 9** (A) Individual spectrum matching results using corrective iterations with the PSD function and the FT approach, (B) corresponding results for the matching of the variability. FT, Fourier Transform; PSD, power spectral density.

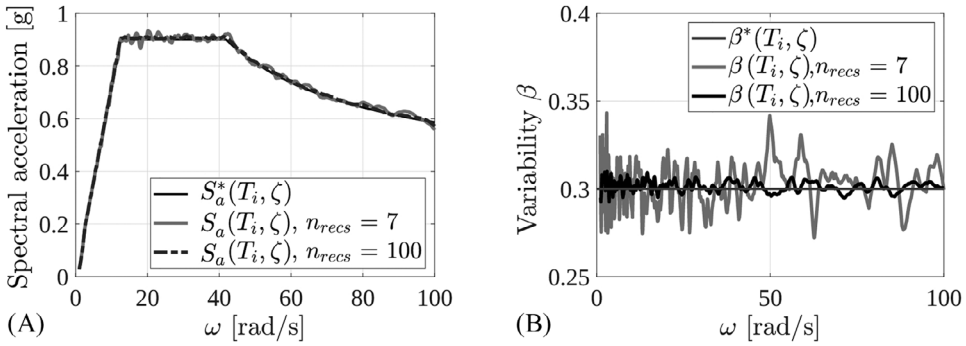


**FIGURE 10** Suite of 7 versus suite of 100 accelerograms: (A) comparison of the mean response spectrum matching, (B) comparison of the matching of the analysis CoV. CoV, Coefficient of Variation.

$S_a^{*j}(T_i,\zeta)$ produced, 10 artificial accelerograms are generated. Subsequently, their response spectra ${S_a}^j(T_i,\zeta)$ are calculated and 5 corrective iterations are performed for every record. Thereafter, the mean squared error between each corrected response spectrum ${S_a}^j(T_i,\zeta)$ and the target spectrum $S_a^{*j}(T_i,\zeta)$ is calculated and finally, the accelerogram whose error is the minimum is selected. The total elapsed time in this case is 3023.19 s ($\approx$ 50 min). In the second suite, only one accelerogram per target spectrum $S_a^{*j}(T_i,\zeta)$ is generated and its response spectrum is subjected to 10 corrective iterations. The total elapsed time in this case is 401.82 s ($\approx$ 7 min). It is obvious that the FT iteration method is significantly faster than the PSD approach. Figure 9 compares the matching achieved with the two iteration approaches. The results of both methods concerning the mean target spectrum are acceptable, however, the FT iterative scheme yields better matching, as it is observed in Figure 9A. Regarding the target variability, the results of the FT approach are much better than the PSD function iteration method (Figure 9B).

The sensitivity of the proposed methodology to the number of ground motions $n$ is also explored, as shown in Figure 10. More specifically, Figure 10 compares the mean spectrum and the analysis variability for suites of 7 and 100 accelerograms. As it is observed, the matching of the mean spectrum is very good for both of the suites. The variability matching is good for the suite of 100 records as expected, however also for the suite of 7 records, the matching is acceptable but requires a higher number of corrective iterations in order to be achieved.

## 4.2 | Second example: Artificial accelerograms generated by the evolutionary spectrum based variant matching a GMM

### 4.2.1 | Target spectra with perfect positive correlation at pairs of periods

A suite of 7, fully non-stationary, accelerograms is sought, and the target mean and variance of the suite are obtained using a GMM. The GMM employed in this study is the BSSA 14[64] model, which provides ground-motion prediction equations for

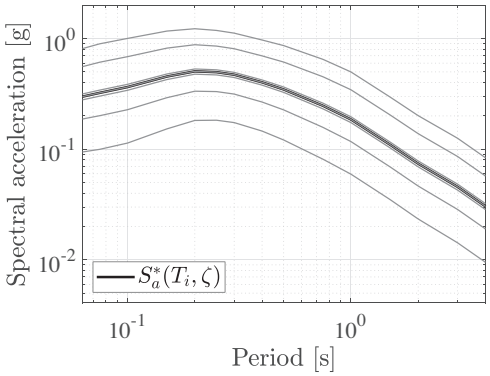


**FIGURE 11** Target response spectra $S_a^{*j}(T_i,\zeta)$ probabilistically produced following Equation (17) for the generation of 7 artificial accelerograms and their median spectrum.

the estimation of the values of the logarithmic mean $\ln\left[S_a{}^{*j}(T_i,\zeta)\right]$ and standard deviation $\sigma^*_{\ln(S_a)}(T_i,\zeta)$ of average horizontal component IMs for shallow crustal earthquakes in active tectonic regions. The region selected in BSSA 14 model is Italy. The seismic scenario considered is of moment magnitude $M_w = 6.5$, Joyner-Boore distance $R_{JB} = 10$ km, and $\varepsilon = 1$. The shear wave velocity averaged over the top 30 m, $V_{S30}$, is set equal to 450 m/s (EC8, soil category "B"), the damping ratio is $\zeta = 5\%$ and the fault type is normal. The target spectra $S_a^{*j}(T_i,\zeta)$ for this example are produced following Equation (17) and are shown in Figure (11). It should be noted that making the comparison between the target spectrum and the spectral mean of the generated accelerograms in logarithmic terms $\ln\left[S_a{}^*(T_i,\zeta)\right]$—as set by equation (16)—includes negative values. Therefore, the comparisons on the following are done between the median target spectra and the median value of the response spectra of the generated accelerograms.[1]

The artificial accelerograms are generated with the evolutionary spectrum based variant discussed in Section 3.2.2. The number of corrective iterations is set to $n_{iter} = 7$. The remaining problem parameters are those of the previous case study. For the significant duration $T_s$, the model proposed by Sandikkaya and Akkar[65] is adopted:

$$\ln T_s = \begin{cases} a_1 + a_2(M_w - 6.5) + a_3(8.5 - M_w)^2 + [a_4 + a_5(M_w - 6.5)]\ln\left(\sqrt{R^2 + a_6^2}\right) + a_7 F_N + a_8 F_R + \\ + a_9 \ln\left[\dfrac{\min(V_{S30}, 1000)}{750}\right] + \epsilon\sigma_{\ln T_s} \end{cases} \tag{30}$$

where $M_w$ is the moment magnitude, $R$ represents source-to-site distance measure (either $R_{epi}$, $R_{hyp}$ or $R_{JB}$), $V_{S30}$ is shear wave velocity averaged over the top 30 m in m/s, $F_N$ and $F_R$ denote the fault type: $F_N$ and $F_R$ are equal to one for normal and reverse faults, respectively, and zero otherwise. The variables $\sigma$ and $\epsilon$ represent the total standard deviation and the number of standard deviations above or below the median estimation, respectively. Parameters $a_i$, where $i = 1, 2 \ldots 9$ are the regression coefficients, obtained as proposed in ref. [65] for the $SD_{5-95}$ model, for $R = R_{JB}$.

For every accelerogram, the significant duration is obtained from the GMM of Equation (30). The variables of the equation are chosen to be compatible with their respective parameters of the BSSA 14 model, that is, $M_w = 6.5$, $R = R_{JB} = 10$ km, fault type normal ($F_N = 1, F_R = 0$), and $V_{S30} = 450$ m/s. The regression coefficients are obtained from ref. [65] for the $SD_{5-95}$ model for $R = R_{JB}$, and are equal to $a_1 = 1.51131$, $a_2 = 1.24873$, $a_3 = 0.04921$, $a_4 = 0.30794$, $a_5 = -0.19161$, $a_6 = 7.5$, $a_7 = 0.06962$, $a_8 = -0.18352$, $a_9 = -0.2957$, and $\sigma = 0.4869$.

Figure 12A compares the median target spectrum obtained from the BSSA 14 GMM with the median value of the response spectrum of the generated accelerograms. Also, Figure 12B shows the matching of the analysis standard deviation to the target. It is observed that, for both the spectral mean and variance, the simulated values are very close to the set target, thus proving the efficiency of the proposed algorithm. Figure 13 shows the mean nonlinear response spectra of the suite of the generated ground motion histories for the case of mean constant strength spectra (Figure 13A) and the case of mean constant ductility spectra (Figure 13B). In both cases, the elastic target spectrum is also shown. It is observed that for the cases of $q_y = 1$ and $\mu = 1$ the resulting spectra are very close to the target, as expected.

[1] Remember that the median of data that follow a lognormal distribution is approximately equal to the mean of the logarithms.

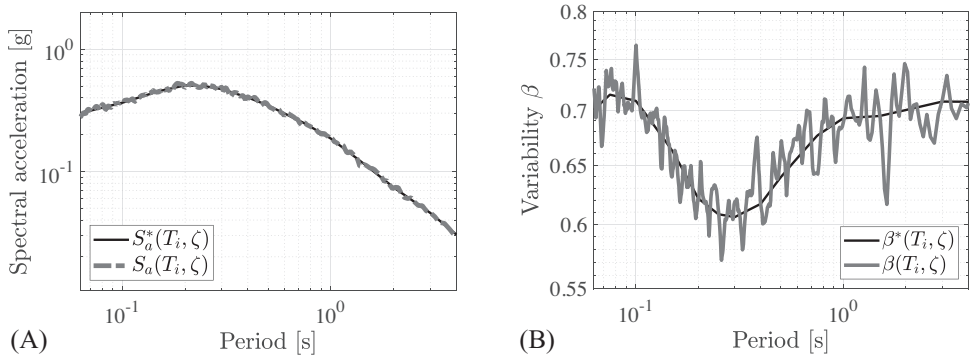


**FIGURE 12** (A) Comparison between the target median response spectrum $S_a^*(T_i,\zeta)$ and the median spectrum $S_a(T_i,\zeta)$ of the generated accelerograms, (B) comparison between the target standard deviation of the natural logarithms $\beta^*(T_i,\zeta) = \sigma^*_{\ln(S_a)}(T_i,\zeta)$ and the obtained $\beta(T_i,\zeta) = \sigma_{\ln(S_a)}(T_i,\zeta)$.

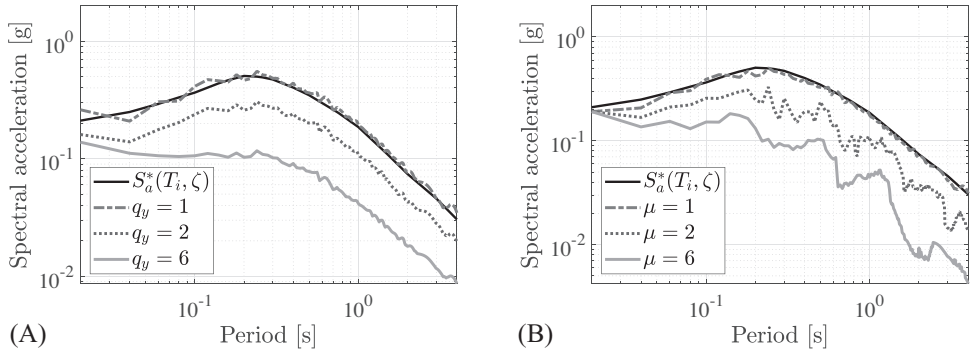


**FIGURE 13** (A) Target elastic response spectrum $S_a^*(T_i,\zeta)$ and mean constant strength spectra for $q_y = 1$, $q_y = 2$, and $q_y = 6$ of the suite of the generated ground motion histories, (B) Target elastic response spectrum $S_a^*(T_i,\zeta)$ and mean constant ductility spectra for $\mu = 1$, $\mu = 2$, and $\mu = 6$ of the suite of the generated ground motion histories.

One of the generated spectrum-compatible accelerograms of the suite is shown in Figure 14, along with its corresponding time-frequency modulating function and its Fourier amplitude plot on the left. The placement of the graphs in the plot of every figure effectively illustrates how the time-frequency function influences both the time and the frequency characteristics. Specifically, the generated accelerogram is aligned parallel to the time axis, visually highlighting the correspondence between the accelerogram's time modulation and the associated time-frequency function. Similarly, the Fourier amplitude of the generated accelerogram is positioned parallel to the frequency axis, visually highlighting the alignment between the accelerogram's frequency modulation and the time-frequency function. Figure 14 shows that generated accelerograms have time-frequency features that have been formed by the proposed time-frequency modulating function of Equation (25). This is confirmed by the fact that the time modulation of the accelerogram is compatible with the shape of the function in the time axis and, at the same time, the frequency modulation follows the shape of the function in the frequency axis. This proves that the accelerograms contained within the suite inherently possess unique time and frequency variations.

### 4.2.2 | Target spectra with specified correlation at pairs of periods

A suite of 20, fully non-stationary, accelerograms is sought, where the generated target spectra account for the correlations between spectral values, and they are produced following Equations (21)–(23). The spectral correlation matrix $\boldsymbol{\rho_{ln}}$ is obtained from the empirical correlation model of Baker and Jayaram,[58] since it is not sensitive to the choice of the GMM that is used to obtain the target median spectrum. In order to achieve enhanced variability matching, the weights for the scoring of Equation (23) are defined as $w_1 = 1.0$, $w_2 = 2.5$, and $w_3 = 0.1$. The number of corrective iterations is set to $n_{iter} = 5$. The remaining problem parameters are those of the application of Section 4.2.1. The generated target spectra

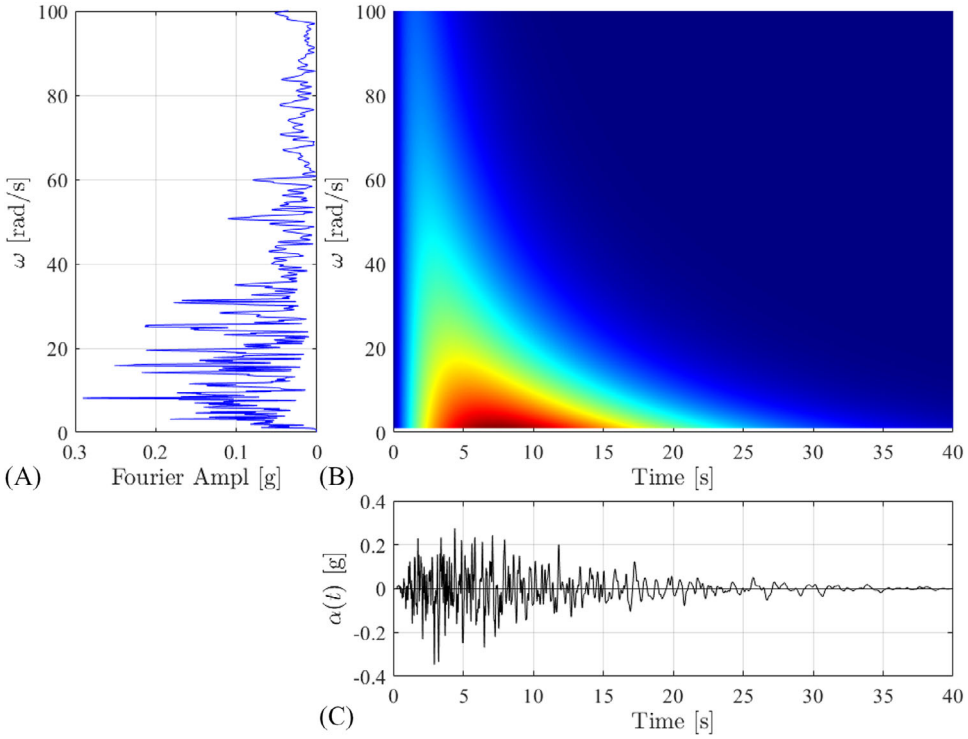


**FIGURE 14** Time-frequency characteristics of the fifth accelerogram from the suite produced in the second example: (A) Fourier amplitude plot, (B) time-frequency modulating function, (C) accelerogram time-history.

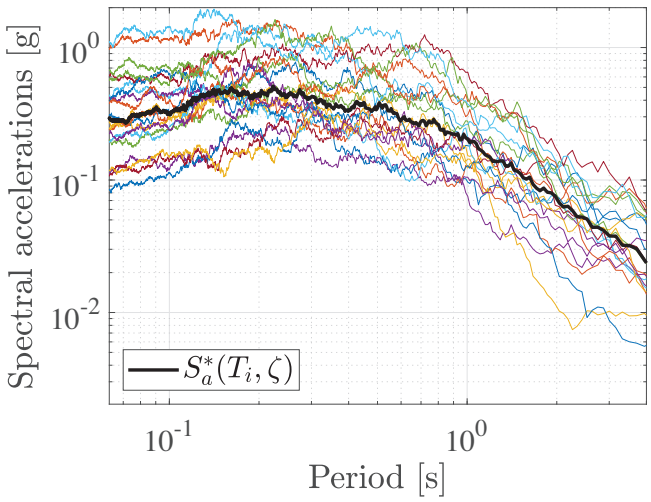


**FIGURE 15** Individual target response spectra $S_a^{*j}(T_i,\zeta)$ probabilistically produced for the generation of 20 artificial accelerograms following Equations (21)–(23) and their respective median spectrum $S_a^*(T_i,\zeta)$.

with spectral correlations, along with their median spectrum are shown in Figure 15. The comparison between the target median response spectrum and the median spectrum of the generated accelerograms is shown in Figure 16A.

Figure 16B shows the analysis standard deviation matching to the target. It is observed that, in general, the generated values are close to the target ones for both spectral ordinates. It is noted that, due to the assumed spectral correlation between periods, additional variability is added within the generated suites of target spectra. Thus, enhanced variability matching like in the case of perfect positive correlation is difficult to achieve, especially for a relatively small number of records. In conclusion, the proposed methodology is efficient and in the case when correlations between pairs of periods are considered.

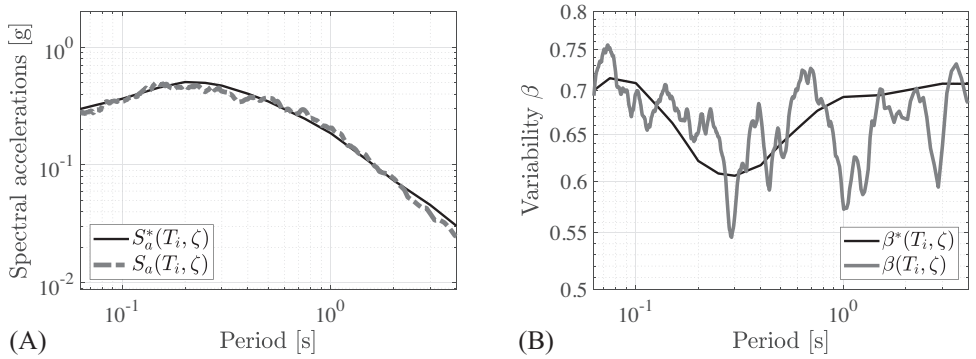


**FIGURE 16** (A) Comparison between the target median response spectrum $S_a^*(T_i,\zeta)$ and the median spectrum $S_a(T_i,\zeta)$ of the generated accelerograms with the spectra of Figure 15, (B) comparison between the target standard deviation of the natural logarithms $\beta^*(T_i,\zeta) = \sigma^*_{\ln(S_a)}(T_i,\zeta)$ and the obtained $\beta(T_i,\zeta) = \sigma_{\ln(S_a)}(T_i,\zeta)$.

## 4.3 | Discussion on the proposed methodology

A discussion on several important aspects that concern advantages, assumptions, as well as potential practical applications of the proposed probabilistic methodology for the stochastic generation of hazard-consistent suites of fully non-stationary seismic records is provided in the following. More specifically, the presented work exhibits a number of noteworthy attributes such as:

i) The generated accelerograms are spectrum-compatible and have a target mean spectrum and target variability, ensuring their seismic-hazard compatibility. Moreover, spectral correlation at pairs of periods can also be considered. Furthermore, the artificial accelerograms are fully non-stationary and have amplitude and frequency modulation features compatible with the site of interest. Compared to relative works available in the literature,[18,19] these features make the proposed methodology highly suitable for everyday applications of engineering practice.
ii) The produced suite of accelerograms contains time-histories that exhibit varying amplitude and frequency modulation features. This element enhances the realistic aspect of the proposed methodology, as past works in the literature produce accelerograms with a fixed power spectrum and modulating function values, resulting in suites of artificial time-histories with very similar time-frequency features.
iii) A new time-frequency modulating function that is compatible with the target time points of the 5% and 95% of the total Arias intensity of the artificial accelerogram is proposed. This feature provides the advantage of generating accelerograms with site-compatible time-frequency modulation characteristics.
iv) The proposed methodology is computationally efficient, whereas its implementation is identified as a straightforward task in Matlab[66] environment.

As a simulating methodology, the proposed work relies on several models and empirically confirmed assumptions. More specifically, the generation of the target spectra is based on the empirically verified observation that the logarithmic spectral accelerations follow the normal distribution, characterized by the mean value and standard deviation. The modeling of the strong motion duration in the *evolutionary spectrum based variant* follows the same observation, and it is sampled as a random variable that follows the log-normal distribution. In the *site and spectrum based variant*, a small number of past-recorded accelerograms are used in order to model the time and the frequency modulation of the artificial accelerograms within the suite. The selected records have to be, preferably, obtained from past seismic activity from the site of interest, or from a site that has similar characteristics. When producing the accelerograms, these records can be simply sampled randomly for every accelerogram. Alternatively, a probabilistic treatment can be applied, however, this would unnecessarily complicate the method, since the proposed methodology aims to extract only the time and frequency modulation characteristics from past records and not other IMs. Finally, it is noted that the basis of the methodology for the generation of fully non-stationary and spectrum-compatible artificial acceleration time-histories relies on the spectral representation method and the use of the power spectrum. Therefore, the phase angles of the produced accelerograms are modeled uniformly distributed over the interval $[0, 2\pi]$.

The study discusses the generation of single-component ground motions, since the proposed model is spectrum-compatible. The methodology can be further extended to generate ground motion signals of two—or three—components. There are several possible ways to extend the proposed methodology for generating two or three component signals. Most GMMs provide the geometric mean response spectrum. Consequently, there are various techniques, like the work of Beyer and Bommer,[67] that allow converting the predictions of geometric mean spectral accelerations of GMMs into different horizontal component definitions. Thus, these methodologies offer a means to define the target spectrum for each component. Regarding the artificial accelerogram generation methods, the *site and spectrum-based variant* benefits from the use of seed records. Consequently, in the case of multidirectional analysis, it is feasible to select multi-component ground motions as seed records, thus including all three components instead of a single component. This allows to indirectly account for the correlations between the components. On the other hand, the *evolutionary spectrum based variant* can rely on the concept of the principal axes of ground motion, originally introduced by Penzien and Watabe[68] and widely adopted in the literature[20]. These principal axes represent an orthogonal set along which the three components are uncorrelated and statistically independent. Thus, the three components can be generated independently as principal components, and then a linear orthogonal transformation by the desired rotation angle can be performed.

Concluding this discussion, it should be emphasized that the proposed methodology aims to offer a practical tool for the everyday needs of engineering practice in a consistent and code-compliant manner. The numerical examples have revealed that although the spectral representation method has a very small inherent variability, the variability of the generated suite can be controlled with enhanced spectrum matching. Furthermore, it was shown that good individual spectrum matching allows to obtain good results even in the case of a database of small size, for example, as in the case of 7 records. Therefore, the proposed methodology can be applied to design problems that employ time-history analyses and follow seismic code criteria. Moreover, the fact that the method achieves compatibility of the produced suite with a target mean spectrum and target variability makes it an efficient tool that can be used in MCS or PBEE applications for the seismic reliability assessment of structures. Additionally, the use and modeling of the power spectrum in both variants makes the methodology easily applicable in stochastic dynamics problems.

## 5 | CONCLUSIONS

A novel, computationally efficient, and practical probabilistic methodology for the stochastic generation of suites of accelerograms has been proposed. The generated accelerograms are fully non-stationary, site-compatible, and have a target mean spectrum and variability. Specified correlation structure at pairs of periods can also be considered. Furthermore, two variants for the generation of suites of artificial accelerograms have been proposed: (i) the site and spectrum based variant where the artificial time-histories are generated using multiple past-recorded ground motions in order to model the non-stationarity in the time-frequency domain, and (ii) the evolutionary spectrum based variant where a time-frequency envelope modifies the PSD function of a stochastic process. A new time-frequency modulating function that ensures site-compatibility has also been proposed. Two illustrative numerical examples have been presented, showing the efficiency of the proposed methodology for both variants. The outcomes, in both approaches, are suites containing non-identical ground motion time-histories whose spectral mean and variability match those obtained from any of the usually employed target spectra in the field of earthquake engineering. Finally, it is noted that the proposed methodology aims to offer a practical tool for everyday engineering applications in a consistent and code-compliant manner, as well as for stochastic dynamics problems.

### ACKNOWLEDGMENTS

The authors gratefully acknowledge the support by the Hellenic Foundation for Research and Innovation (Grant No. 1261).

### DATA AVAILABILITY STATEMENT

The data that support the findings of this study are available in GitHub at https://github.com/HeraYanni/ProbGenArtifAccel.git. These data were derived from the following resources available in the public domain: - GitHub, https://github.com/HeraYanni/ProbGenArtifAccel.git

### ORCID

*Hera Yanni* https://orcid.org/0009-0003-0314-0519
*Michalis Fragiadakis* https://orcid.org/0000-0002-0698-822X

*Ioannis P. Mitseas* https://orcid.org/0000-0001-5219-1804

## REFERENCES


1. CEN. Eurocode 8: Design of structures for earthquake resistance. Part I: General rules, seismic actions and rules for buildings (EN1998-1). European Committee for Standardization, Brussels; 2004.
2. ASCE. ASCE/SEI 7-22: Minimum Design Loads and Associated Criteria for Buildings and Other Structures. American Society of Civil Engineers, Reston, VA; 2021.
3. Jayaram N, Lin T, Baker J. A Computationally efficient ground-motion selection algorithm for matching a target response spectrum mean and variance. *Earthquake Spectra*. 2011;27:797-815.
4. Grigoriou M. Do seismic intensity measures (IMs) measure up? *Probab Eng Mech*. 2016;46:80-93.
5. Dávalos H, Miranda E. Evaluation of bias on the probability of collapse from amplitude scaling using spectral-shape-matched records. *Earthquake Eng Struct Dyn*. 2019;48:970-986.
6. Baker J, Lee C. An improved algorithm for selecting ground motions to match a conditional spectrum. *J Earthquake Eng*. 2018;22:708-723.
7. Georgioudakis M, Fragiadakis M. *Selection and scaling of ground motions using multicriteria optimization*. ASCE. 2020;146.
8. Boore DM. Simulation of ground motion using the stochastic method. *Pure Appl Geophys*. 2003;160:635-676.
9. Motazedian D, Atkinson GM. Stochastic finite-fault modeling based on a dynamic corner frequency. *Bull Seismol Soc Am*. 2005;95:995-1010.
10. Rezaeian S, DerKiureghian A. A stochastic ground motion model with separable temporal and spectral nonstationarities. *Earthquake Eng Struct Dyn*. 2008;37:1565-1584.
11. Lin YK. On random pulse train and its evolutionary spectral representation. *Probab Eng Mech*. 1986;1:219-223.
12. Conte JP, Pister KS, Mahin SA. Nonstationary ARMA modeling of seismic motions. *Soil Dyn Earthquake Eng*. 1992;11:411-426.
13. Shinozuka M, Deodatis G. Simulation of stochastic processes by spectral representation. *Appl Mech Rev*. 1991;44:191-204.
14. Baglio M, Cardoni A, Cimellaro GP, Abrahamson N. Generating ground motions using the Fourier amplitude spectrum. *Earthquake Eng Struct Dyn*. 2023;52(15):4884-4899.
15. Wang D, Fan Z, Hao S, Zhao D. An evolutionary power spectrum model of fully nonstationary seismic ground motion. *Soil Dyn Earthquake Eng*. 2018;105:1-10.
16. Sabetta F, Pugliese A, Fiorentino G, Lanzano G, Luzi L. Simulation of non-stationary stochastic ground motions based on recent Italian earthquakes. *Bull Earthquake Eng*. 2021;19:3287-3315.
17. Ni SH, Xie WC, Pandey MD. Generation of spectrum-compatible earthquake ground motions considering intrinsic spectral variability using Hilbert–Huang transform. *Struct Saf*. 2013;42:45-53.
18. Cacciola P, Zentner I. Generation of response-spectrum-compatible artificial earthquake accelerograms with random joint timefrequency distributions. *Probab Eng Mech*. 2012;28:52-58.
19. Zentner I. A procedure for simulating synthetic accelerograms compatible with correlated and conditional probabilistic response spectra. *Soil Dyn Earthquake Eng*. 2014;63:226-233.
20. Rezaeian S, DerKiureghian A. Simulation of orthogonal horizontal ground motion components for specified earthquake and site characteristics. *Earthquake Eng Struct Dyn*. 2012;41(2):335-353.
21. Huang D, Wang Z. Wavelet-based stochastic model for jointly simulating three-component ground motions. *Bull Seismol Soc Am*. 2022;112(3):1483-1501.
22. Housner GW. Characteristics of strong-motion earthquakes. *Bull Seismol Soc Am*. 1947;37:19-31.
23. Vanmarcke EH. *Developments in Geotechnical Engineering: Chapter 8 - Structural Response to Earthquakes*. Elsevier; 1976. ISBN 9780444414946.
24. Vanmarcke EH, Gasparini DA. Simulated Earthquake Ground Motions. *K - Seismic Response Analysis of Nuclear Power Plant Systems K1 - Ground Motion and Design Criteria SMiRT 4*. 1977.
25. Cacciola P, Colajanni P, Muscolino G. Combination of modal responses consistent with seismic input representation. *J Struct Eng*. 2004;130:47-55.
26. Kanai K. Semi-empirical formula for the seismic characteristics of the ground. *Bulletin of the Earthquake Research Institute, University of Tokyo*. 1957;35:309-325.
27. Tajimi H. A statistical method of determining the maximum response of a building structure during an earthquake. *Proc. 2nd WCEE*. 1960:781-797.
28. Clough RW, Penzien J. *Dynamics of Structures*. Mc Graw-Hill; 1975.
29. Spanos P, Loli LV. A statistical approach to generation of design spectrum compatible earthquake time histories. *Inter J Soil Dyn Earthquake Eng*. 1985;4:2-8.
30. Iervolino I, Luca FD, Cosenza E. Spectral shape-based assessment of SDOF nonlinear response to real, adjusted and artificial accelerograms. *Eng Struct*. 2010;32:2776-2792.
31. Beck J, Papadimitriou C. Moving resonance in nonlinear response to fully nonstationary stochastic ground motion. *Probab Eng Mech*. 1993;8:157-167.
32. Tubaldi E, Kougioumtzoglou IA. Nonstationary stochastic response of structural systems equipped with nonlinear viscous dampers under seismic excitation. *Earthquake Eng Struct Dyn*. 2015;44:121-138.
33. Mitseas IP, Kougioumtzoglou IA, Spanos PD, Beer M. Nonlinear MDOF system survival probability determination subject to evolutionary stochastic excitation. *Strojniški vestnik - J Mech Eng*. 2016;62:440-451.

34. Jennings PC, Housner GW, Tsai NC. Simulated earthquake motions. *Tech. rep., EERL California Institute of Technology*. 1968.
35. Saragoni GR, Hart GC. Simulation of artificial earthquakes. *Earthquake Eng Struct Dyn*. 1973;2:249-267.
36. Genovese F, Biondi G, Cascone E, Muscolino G. Energy-compatible modulating functions for the stochastic generation of fully non-stationary artificial accelerograms and their effects on seismic site response analysis. *Earthquake Eng Struct Dyn*. 2023;52:2682-2707.
37. Preumont A. The generation of non-separable artificial earthquake accelerograms for the design of nuclear power plants. *Nucl Eng Des*. 1985;88:59-67.
38. Spanos PD, Failla G. Evolutionary spectra estimation using wavelets. *J Eng Mech*. 2004;130:952-960.
39. Cacciola P. A stochastic approach for generating spectrum compatible fully nonstationary earthquakes. *Comput Struct*. 2010;88:889-901.
40. Ferreira F, Moutinho C, Cunha A, Caetano E. An artificial accelerogram generator code written in Matlab. *Eng Rep*. 2020;2:e12129.
41. Fragiadakis M, Lagaros ND. An overview to structural seismic design optimisation frameworks. *Comput Struct*. 2011;89(11):1155-1165.
42. Song C, Kawai R. Monte Carlo and variance reduction methods for structural reliability analysis: a comprehensive review. *Probab Eng Mech*. 2023;73:103479.
43. Kougioumtzoglou IA, Ni P, Mitseas IP, Fragkoulis VC, Beer M. An approximate stochastic dynamics approach for design spectrum based response analysis of nonlinear oscillators with fractional derivative elements. *Int J Non Linear Mech*. 2022;146:104178.
44. Mitseas IP, Beer M. Modal decomposition method for response spectrum based analysis of nonlinear and non-classically damped systems. *Mech Syst Sig Process*. 2019;131:469-485.
45. Mitseas IP, Beer M. Fragility analysis of nonproportionally damped inelastic MDOF structural systems exposed to stochastic seismic excitation. *Comput Struct*. 2020;226:106129.
46. Mitseas IP, Beer M. First-excursion stochastic incremental dynamics methodology for hysteretic structural systems subject to seismic excitation. *Comput Struct*. 2021;242:106359.
47. Fragiadakis M, Diamantopoulos S. Fragility and risk assessment of freestanding building contents. *Earthquake Eng Struct Dyn*. 2020;49:1028-1048.
48. Abbiati G, Broccardo M, Abdallah I, Marelli S, Paolacci F. Seismic fragility analysis based on artificial ground motions and surrogate modeling of validated structural simulators. *Earthquake Eng Struct Dyn*. 2021;50:2314-2333.
49. Psycharis IN, Fragiadakis M, Stefanou I. Seismic reliability assessment of classical columns subjected to near-fault ground motions. *Earthquake Eng Struct Dyn*. 2013;42:2061-2079.
50. Zacharenaki A, Fragiadakis M, Assimaki D, Papadrakakis M. Bias assessment in incremental dynamic analysis due to record scaling. *Soil Dyn Earthquake Eng*. 2014;67:158-168.
51. Fragiadakis M, Vamvatsikos D. Fast performance uncertainty estimation via pushover and approximate IDA. *Earthquake Eng Struct Dyn*. 2010;39:683-703.
52. Yanni H, Fragiadakis M, Mitseas IP. A novel method for the stochastic generation of artificial accelerograms. In: Proceedings of the 5th Panhellenic Conference on Earthquake Engineering and Engineering Seismology. Hellenic Association for Earthquake Engineering; 2022.
53. Yanni H, Fragiadakis M, Mitseas IP. A novel stochastic methodology for the generation of artificial seismic accelerograms. In: Proceedings of the EURODYN 2023 XII International Conference on Structural Dynamics. European Association for Structural Dynamics; 2023.
54. Vanmarcke EH. Properties of spectral moments with applications to random vibration. *J Eng Mech Div*. 1972;98:425-446.
55. DerKiureghian A. structural response to stationary excitation. *J Eng Mech Div*. 1980;106:1195-1213.
56. Kramer SL. *Geotechnical Earthquake Engineering*. Prentice-Hall International Series in Civil Engineering and Engineering Mechanics. Prentice-Hall; 1996.
57. Tarbali K, Bradley BA. Ground motion selection for scenario ruptures using the generalised conditional intensity measure (GCIM) method. *Earthquake Eng Struct Dyn*. 2015;44(10):1601-1621.
58. Baker JW, Jayaram N. Correlation of spectral acceleration values from NGA ground motion models. *Earthquake Spectra*. 2008;24(1):299-317.
59. Luzi L, Lanzano G, Felicetta C, et al. Engineering Strong Motion Database (ESM) (Version 2.0). Istituto Nazionale di Geofisica e Vulcanologia (INGV). 2020.
60. PEER (Pacific Earthquake Engineering Research Center). Shallow crustal earthquakes in active tectonic regimes. https://ngawest2.berkeley.edu/site
61. US-NRC. Regulatory Guide 1.208 [electronic resource]: a performance-based approach to define the site-specific earthquake ground motion. 2007. Accessed 12 July, 2023. https://www.nrc.gov/docs/ML0703/ML070310619.pdf
62. Bradley BA. A generalized conditional intensity measure approach and holistic ground-motion selection. *Earthquake Eng Struct Dyn*. 2010;39:1321-1342.
63. Boore DM, Bommer JJ. Processing of strong-motion accelerograms: needs, options and consequences. *Soil Dyn Earthquake Eng*. 2005;25:93-115.
64. Boore DM, Stewart JP, Seyhan E, Atkinson GM. NGA-West2 Equations for Predicting PGA, PGV, and 5% Damped PSA for Shallow Crustal Earthquakes. *Earthquake Spectra*. 2014;30:1057-1085.
65. Sandıkkaya MA, Akkar S. Cumulative absolute velocity, Arias intensity and significant duration predictive models from a pan-European strong-motion dataset. *Bull Earthquake Eng*. 2017;15:1881-1898.
66. MathWorks. MATLAB version 2021a [Computer Program]. https://www.mathworks.com/products/matlab.html

67. Beyer K, Bommer JJ. Relationships between median values and between aleatory variabilities for different definitions of the horizontal component of motion. *Bull Seismol Soc Am*. 2006;96(4A):1512-1522.
68. Penzien J, Watabe M. Characteristics of 3-dimensional earthquake ground motions. *Earthquake Eng Struct Dyn*. 1975;3:365-373.

**How to cite this article:** Yanni H, Fragiadakis M, Mitseas IP. Probabilistic generation of hazard-consistent suites of fully non-stationary seismic records. *Earthquake Engng Struct Dyn*. 2024;53:3140–3164. https://doi.org/10.1002/eqe.4153